CDF/MEMO/TRIGGER/PUBLIC/5534
May 29, 2001

A Study of SVT Performance on Multijet Events for the Higgs Search: Background Rejection and Timing Issues

Giovanni Busetto, Giorgio Cortiana,
Tommaso Dorigo, Luca Scodellaro, Virginia de Grivel

Padova University and INFN

Abstract

We present a proposal for a Run II multijet trigger aimed at selecting $H^0 + Z^0/W^\pm \rightarrow 4\ jet$ events via a tagging of the particles produced in the decays of b or c quarks. These tools are meant to be efficient for Higgs masses up to $\sim 130\ GeV/c^2$, where $H^0 \rightarrow b\bar{b}$ is the dominant decay process.
In this note we focus mainly on the SVT performance in reconstructing displaced tracks in HV events, and in discriminating these events from the QCD background; we also discuss how the noise in the silicon strips and the processing time needed at trigger Level 2 for these complicated events will affect the performance.
Finally, we discuss briefly some possible Level 3 requirements on the events passing the Level 2 selection.

1 Introduction

One of the primary goals for Run II at the TEVATRON is the search for the Higgs boson. Studies based on Run II simulations show that, for an integrated (CDF and D0) luminosity of the order of $10fb^{-1}$, a 3σ H^0 evidence is at reach for $M_{\mathrm{H}} \lesssim 130GeV/c^2$, while a 95% C.L. exclusion is achievable for $M_{\mathrm{H}} \lesssim 190GeV/c^2$ [1].

Although Higgs production at the TEVATRON is dominated by gluon fusion ($\sigma \sim 0.7pb$ for $M_{\mathrm{H}} = 120GeV/c^2$), its associated production with a vector boson is a much more promising channel despite its lower cross-section ($\sigma \sim 0.3pb$ for $M_{\mathrm{H}} = 120GeV/c^2$), since it allows a much more effective control of the QCD background by the vector boson reconstruction.

Experimentally, the most promising final states correspond to leptonic decays of the vector bosons, since isolated high P_T leptons provide a good trigger and a clean signature; however, they are affected by a limited branching ratio ($\sim 11\%$). Conversely, final states with hadronically decaying vector bosons are characterized by a higher branching ratio ($\sim 47\%$), but suffer from multijet backgrounds which several orders of magnitude larger.

In both cases, however, since for $M_{\mathrm{H}} \lesssim 130GeV/c^2$ the favoured Higgs decay channel proceeds through $b\bar{b}$ production ($B.R. \sim 70\%$), b-jet identification is a crucial feature for reducing backgrounds; two approaches can be pursued: the first one consists of tagging the soft leptons produced in the semileptonic decay of the B hadrons and is complemental with the second one, which, on the other hand, is based on the reconstruction of the secondary vertex due to the large B-hadron lifetime.

The Silicon Vertex Tracker (SVT) has been designed to provide a fast identification of displaced tracks candidates to come from a secondary vertex, in time for a Level 2 trigger decision, and it has recently demonstrated its ability to reconstruct tracks online during the commissioning run[2]. However, the hardware has been optimized as a B-physics-specific tool[3], and its tracking capability has been demonstrated only for the low-P_T b-production events most interesting for B physics.

The main purpose of this note is to study the SVT performance in a multijet environment typical of $HV \rightarrow 4jet$ events. In Section 2 we introduce briefly the datasets and the simulation used for all our studies. In Section 3 we discuss the calorimetric requirements we ask at Level 1 and 2. In Section 4 we estimate the performance of SVT in reconstructing displaced tracks in HV events, and in discriminating these events from the QCD background; we also discuss how noise in the silicon strips will affect the performance, and we estimate the processing time needed at trigger Level 2 for these complicated events. In Section 5 we introduce some studies for Level 3 requirements. Finally, in Section 6 we draw some conclusions.

2 The Generation and the Simulation of the Datasets

2.1 Generation of signal and background events

We used the 3.12.2 release of the Run II offline for our simulation of VH events. PYTHIA V6.129 + QQ V9.1 with the CTEQ3M PDF set was used to generate the signal events (MSEL = 17); CDF2SIM was used to perform a full simulation of the CDF II detector. The Higgs boson mass was set at 120 GeV/c^2, and the creation of a multijet final state was induced by forcing hadronic decays of the W and Z bosons, and $b\bar{b}$ decays of the Higgs. Four samples were generated to scan four different values of the fraction of noisy strips in the silicon detector[1]: 0.0%, 0.5% (2000 events), 1.0% and 2.0% (1500 events) (see Sec. 4.4).

Furthermore, some samples of QCD $2 \to 2$ processes (ISUB = 11, 12,13, 28,53 and 68) were generated using PYTHIA V6.129 + QQ V9.1 with the MRSD- PDF set and simulated with CDF2SIM: four samples selected with Level 1 requirements (see Sec. 3) for timing studies ($\sim$ 5000 events with noise level set to 0.5% and $\sim$ 1000 events with noise level set to 0.0%, 1.0% and 2.0% respectively), and four samples filtered with Level 2 calorimetric requirements to test the SVT performance in background rejection ($\sim$ 700 events with noise level set to 0.5% and $\sim$ 300 events with noise level set to 0.0%, 1.0% and 2.0% respectively).

2.2 The simulation

To simulate the action of SVT on these events we used a stand-alone simulation written by G. Punzi, SVTSIM. This program accepts as input a list of hit positions in the silicon strips per each event, along with azimuthal angle and curvature of each track identified by the XFT processor[2], and simulates in detail pattern recognition and track fitting[3], working out the SVT response in the form of a list of identified tracks, along with hits position, azimuthal angle at the origin, curvature, and impact parameter of each. The task of finding silicon hits and producing the ASCII file to be input to the SVT simulation is assigned to a custom module, DUMPSVT, to avoid the need to dump on disk huge files containing raw ADC counts[4].

The SVT simulation is used in the so-called "4/4" AM mode, where at least one hit is required in each of four silicon layers in order to reconstruct a track in a given SVX II sector[5]. The four input layers can be chosen among the five SVX II layers plus layer 00. Depending on the combination of chosen planes, a suitable set of patterns has to be fed into the simulation[6]. For our studies we used the standard choice of L0, L1, L2 and L3 as input planes; we therefore did not investigate the improvements in impact parameter resolution which may be possible by substituting one of those layers with L00, or, conversely, the probable reduction of fake tracks when using layer 4 as a substitute of one of the inner layers[7]. These improvements may be the subject of a future study. Other details of the

[1]We simulate hits in the silicon microstrips using Padova's charge deposition model[4]. Random noise is added to the silicon strips such that a user-defined fraction of these yields a signal above the ADC threshold. Of course, this random addition of charge also impacts the reconstructed position of the centroid of clusters due to real particles.

[2]The user can choose to provide the output of a full offline reconstruction of COT tracks as an alternative to the XFT output. That allows for efficiency and systematics studies.

[3]The user can choose whether to use the real linearized fit performed by the hardware boards or an idealized regular fit. This is useful when dealing with configurations for which the linearized fit constants have not been computed yet.

[4]The code converting the SVXD banks and the XFT/COT output to a suitable ASCII file, containing the computed centroids of hit clusters plus the XFT coordinates was provided by P. Gatti and updated to 3.12.2 release.

[5]We use a terminology where a SVX II sector identifies a half-barrel and 30 degrees in azimuth: there is thus a total of 72 such sectors.

[6]These patterns have been generated by G. Chlachidze.

[7]It appears that L4 strips are on average much less noisy than the L3 ones (N. Bacchetta, private

chosen configuration involve the superstrip size[8], which was set to $300\mu m$, and the number of patterns stored in each memory bank, set to 32,768. The default value of the cut on the fit χ^2 was set at 12.6, but this latter figure was later varied to study its effect on our datasets.

The output of SVTSIM is stored in PAW ntuples that are dumped in ASCII files and are input with the original file from DUMPSVT to a C++ module that merges all this information with some variables from generation, trigger and offline Levels. In particular, we use the CALTRIGGER package to simulate the calorimetric trigger.

3 Level 1 and Level 2 Calorimetric Requirements

In a precedent version of this note we showed Level 2 acceptances after the application of cuts on the SVT output without simulating Level 1 and the calorimetric Level 2 requirements. In this version, all studies will be repeated after Level 1 and Level 2 simulation.

Calorimetric requirements for collecting HV decays in the multijet channel have been recently proposed [5], in order to increase the efficiency of the Run I multijet trigger, which was not optimized for the Higgs search [6].

The Level 1 calorimetric primitive has been taken from the QCD inclusive JET70 path, which requires a single inclusive trigger tower with $E_T \geqslant 10\ GeV$. The signal efficiency after this requirement is $\gtrsim 98\%$, while the rate has been estimated to be 2.7 kHz (for $\mathcal{L} = 10^{32} cm^{-2} s^{-1}$) [7].

The choice of the optimal Level 2 primitive is performed on the basis of efficiency maximization. $HV \to had$ events are expected[9] to produce four jets in the final state; taking into account the chance of losing one jet or merging two of them, the requirement of only three clusters at Level 2 has been established, obtaining a significant increase in the efficiency (see Fig. 3). After the behaviour of different combinations of ΣE_T^{cl} primitives and cluster E_T thresholds has been studied, the following requirements have been established:

$$E_T^{cl} \geqslant 10\ GeV,\ N_{cl} \geqslant 3,\ \Sigma E_T^{10} \geqslant 90\ GeV,$$

corresponding to an efficiency of $\sim 78\%$ and a rate of 15.4 Hz.

To study timing issues, we consider also the possibility to use a Level 1 trigger requiring two central trigger towers with $E_T \geqslant 5\ GeV$ and two XFT tracks with $P_T \geqslant 2\ GeV/c$ [8]; such a requirement yields a signal efficiency of $\sim 94\%$ and a rate of 2.7 kHz at Level 1 and a signal efficiency of $\sim 76\%$ and a rate of 13.6 Hz at Level 2.

These results have been obtained by running the RUN2TRS package on a signal Monte Carlo[5] and on Run I JET20 data. A comparison with the prediction of Run II CALTRIGGER package is proposed in Figs. 1 to 4: a clear difference appears, due to the not optimized calibration of the calorimetric simulation in CDF2SIM. As a consequence, the nominal calorimetric requirements will be tighter than estimed above. We will have to allow for this effect when we discuss the SVT performance.

communication). Of course, layer 4 is also expected to have a lower occupancy than the inner layers.

[8] In order to reduce the memory requirements of the associative memory banks, where all possible hit patterns are stored, groups of a few neighboring silicon microstrips (five in this case) are merged into superstrips.

[9] Disregarding initial and final state radiation processes at this time.

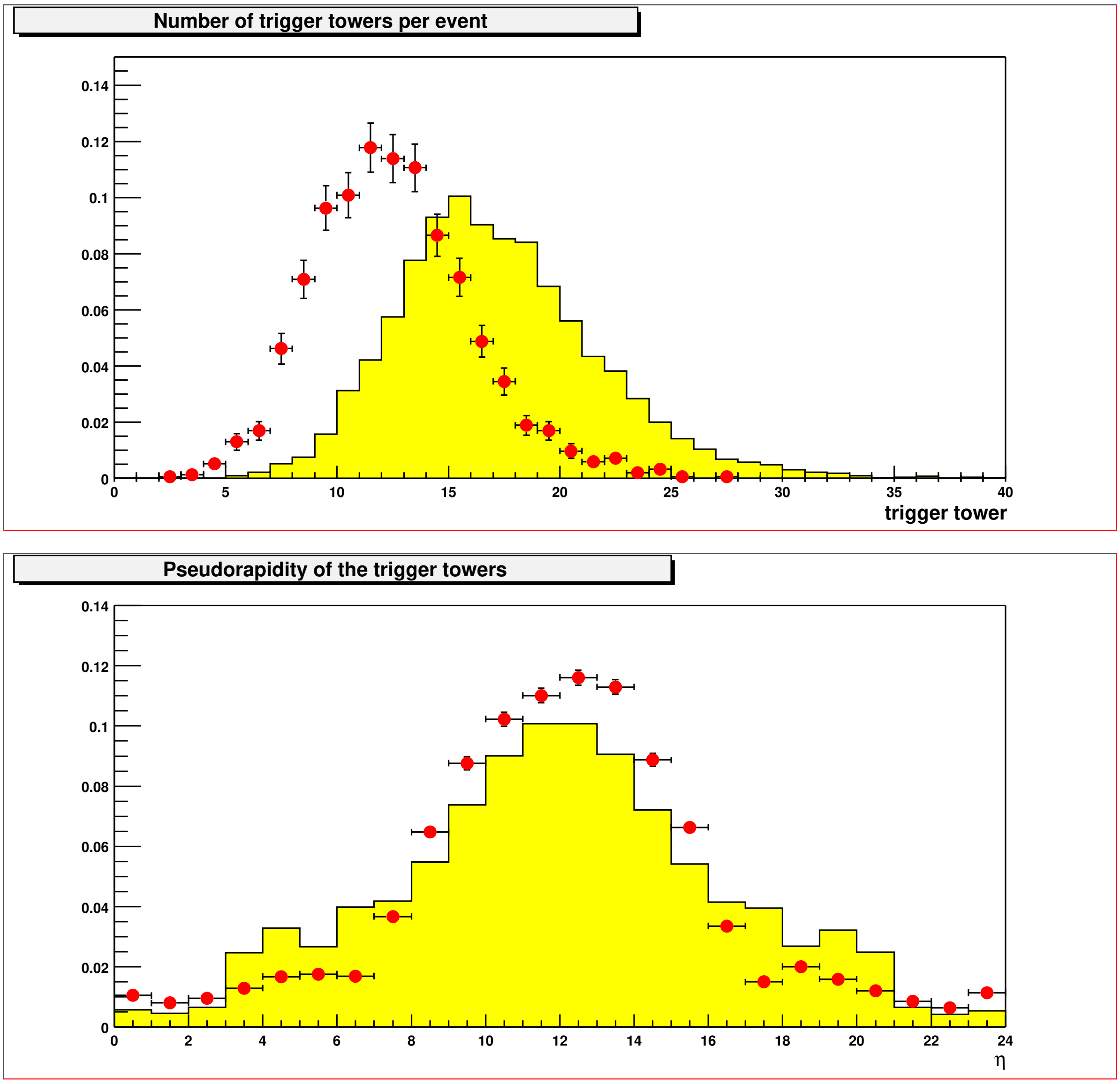

Figure 1: *Comparison between calorimetric variables as predicted by* RUN2TRS *(histograms) and* CALTRIGGER *(full red circles) packages. HV events are used. Top: trigger tower multiplicity (a threshold of 2 GeV in E_T is required). Bottom: trigger tower pseudorapidity.*

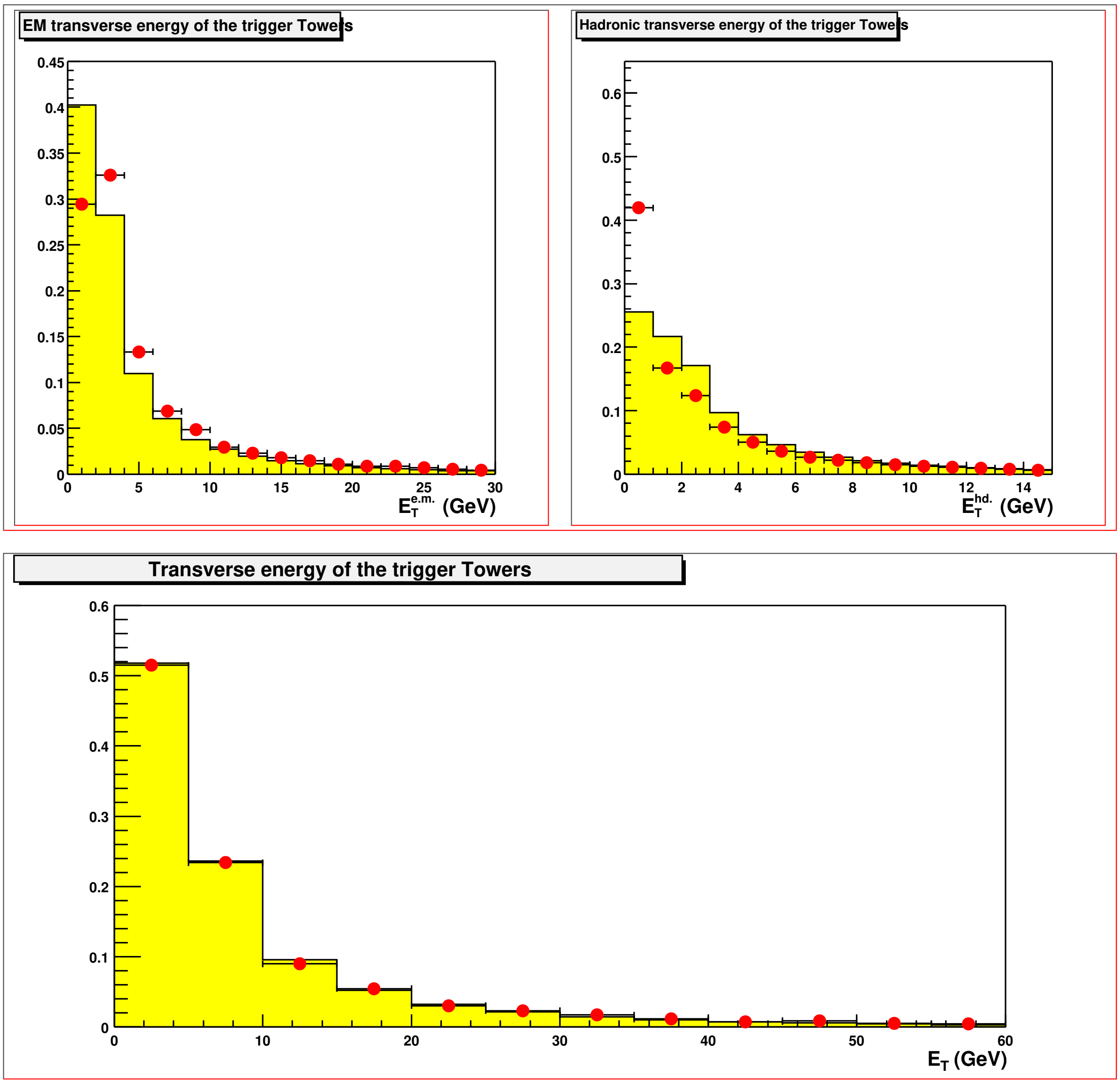

Figure 2: *Comparison between transverse energy of the trigger towers as predicted by* RUN2TRS *(histograms) and* CALTRIGGER *(full red circles) packages. HV events are used. Top left: transverse energy in the electromagnetic calorimeter. Top right: transverse energy in the hadronic calorimeter. Bottom: total transverse energy.*

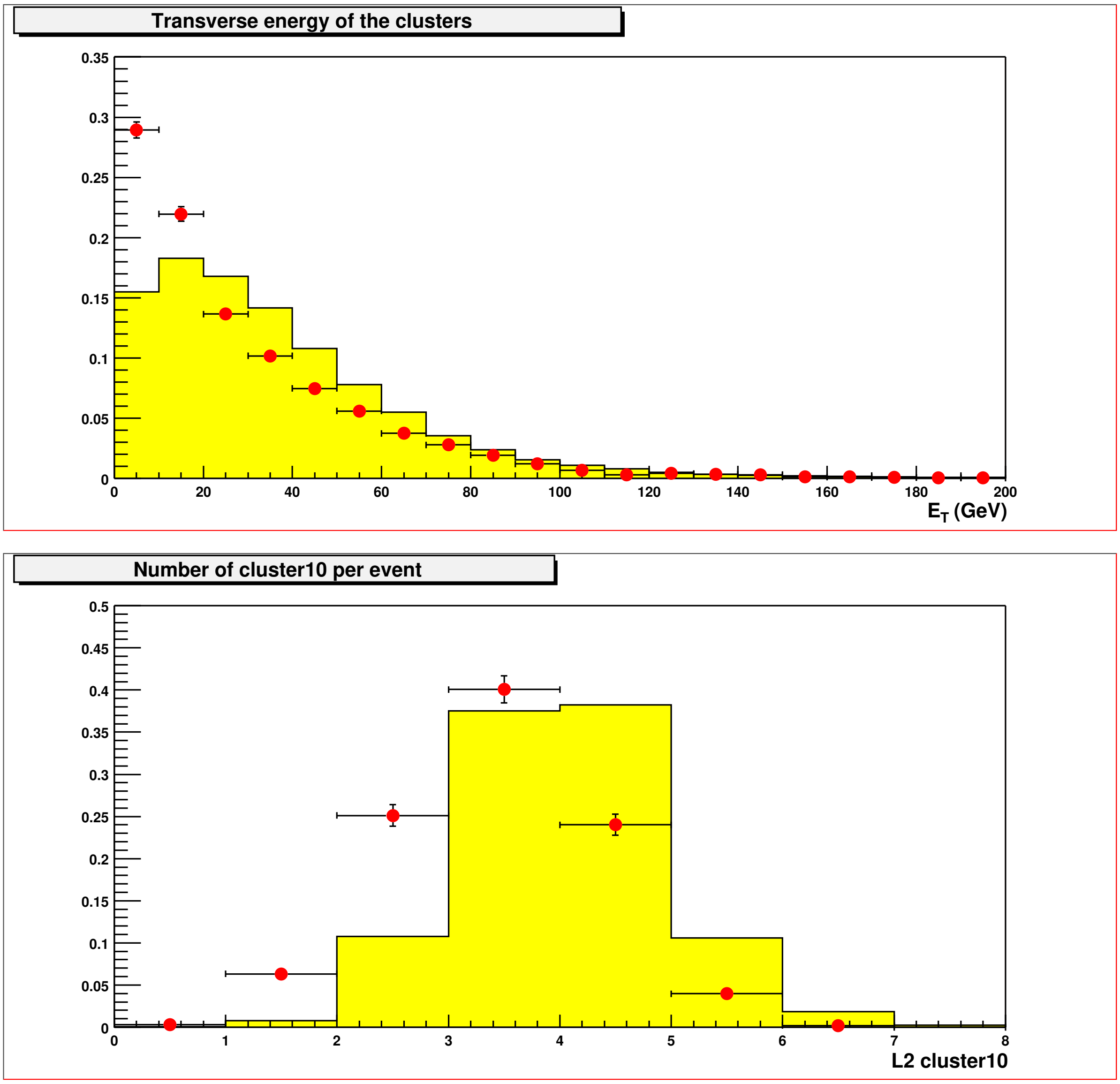

Figure 3: *Comparison between calorimetric variables as predicted by* RUN2TRS *(histograms) and* CALTRIGGER *(full red circles) packages. HV events are used. Top: transverse energy of the Level 2 clusters. Bottom: cluster multiplicity (a threshold of* 10 *GeV in E_T is required). No Level 1 requirement is applied.*

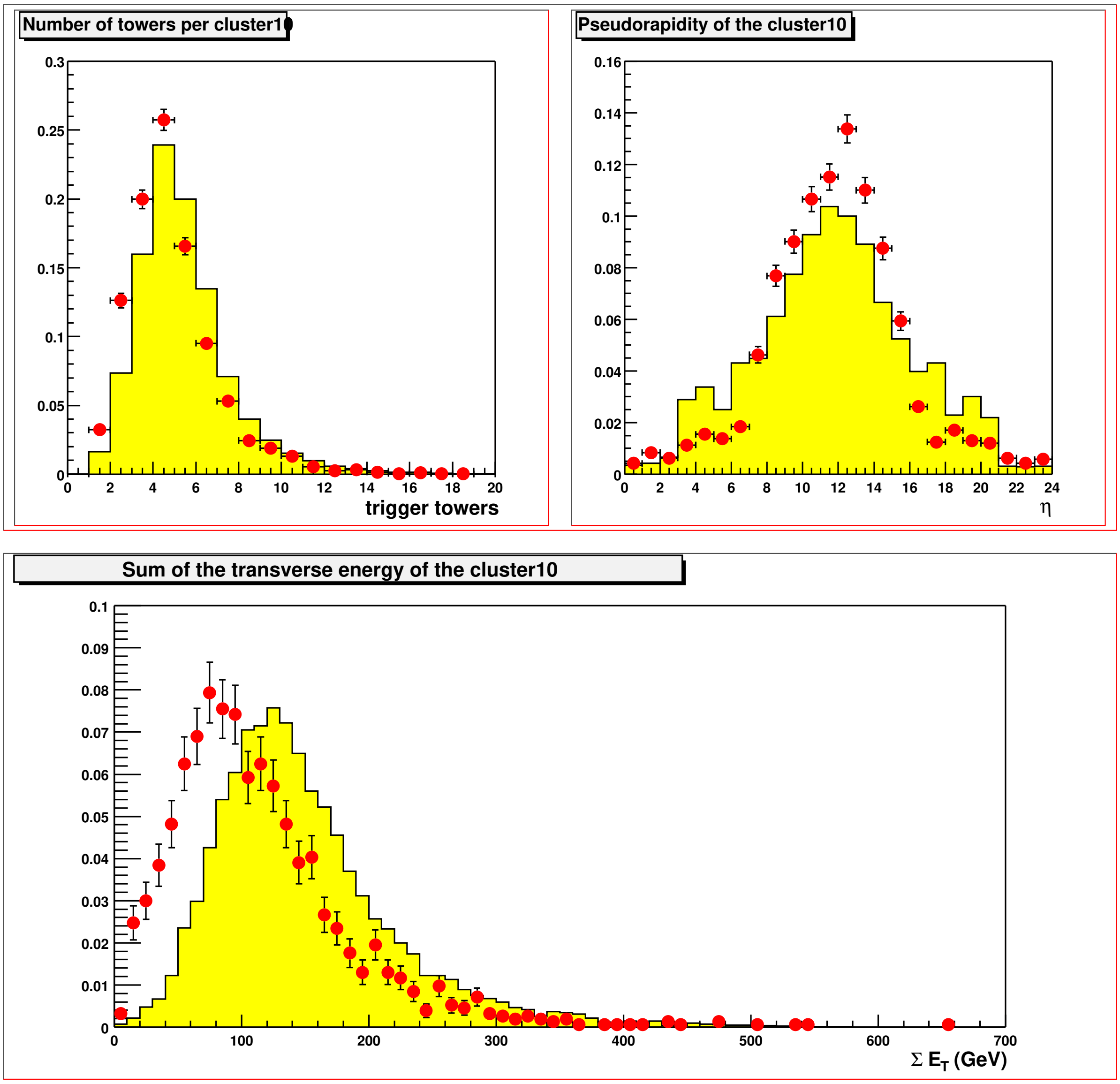

Figure 4: *Comparison between calorimetric variables as predicted by* RUN2TRS *(histograms) and* CALTRIGGER *(full red circles) packages. HV events are used. Top left: trigger tower multiplicity in the Level 2 clusters (a threshold of* 10 *GeV in E_T is required). Top right: cluster pseudorapidity. Bottom: Sum of the cluster E_T. No Level 1 requirement is applied.*

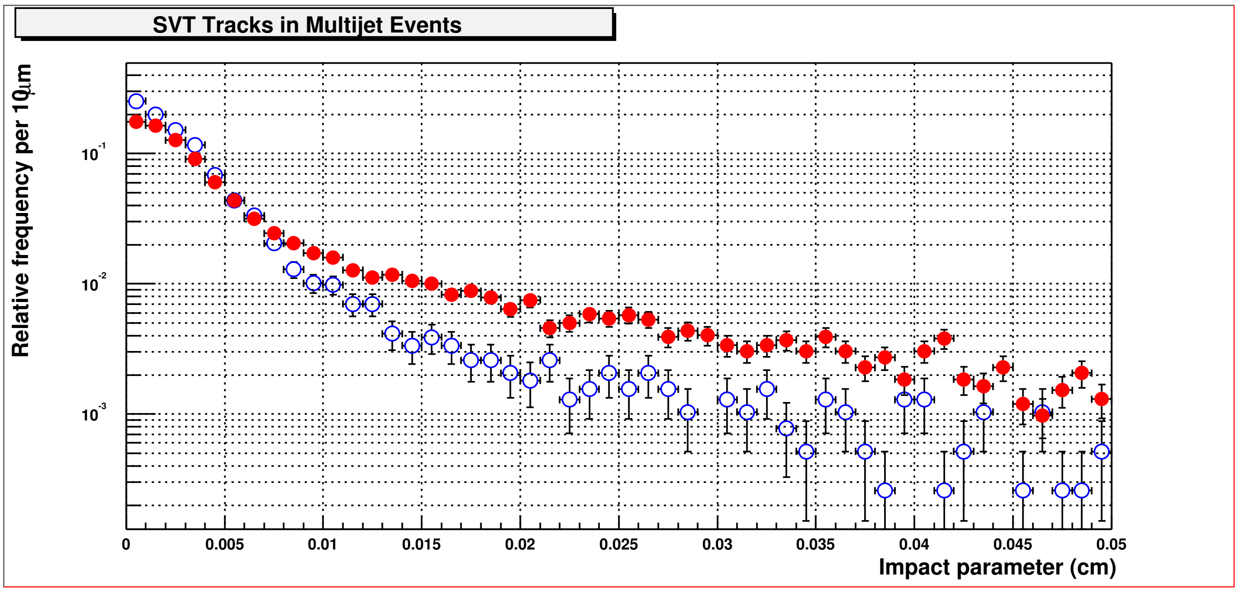

Figure 5: *Impact parameter distribution of good SVT tracks in multijet events, for the default simulation (0.5% of noisy silicon strips, χ^2 cut set at 12.6). In blue (open circles) tracks in QCD events; in red (full circles) tracks in HV events.*

4 SVT

When discussing the possibility of using the SVT output for the selection of a high-P_T process such as associated VH production (where V denotes a W or Z boson), one needs to first ascertain that these events are indeed reconstructable by SVT, given the proposed settings of the device, the available information, and the decision time at trigger Level 2. That is what we set out to do in the following.

4.1 Preselection of good SVT tracks

Reconstructed tracks passing the χ^2 cut and with a P_T greater than 2.0 GeV/c are the output of SVT: for each track, impact parameter (d), curvature (c), and azimuthal angle at the origin (ϕ_0) are available to the Level 2 processors. However, knowledge of the functioning of the XFT processor may allow a cleanup of this set of data, as is explained below.

XFT yields to the SVT hit finders and mergers two numbers per track: the curvature and the azimuthal position at the radius of the third axial superlayer (SL 6). Although the latter is measured with a precision of 0.156 degrees, no more than one track is considered through each of 288 azimuthal slices, each 1.25 degrees wide. This information can be used with success in combination with the SVT output, particularly in the case of a very crowded and/or noisy environment: SVT has in fact the freedom to use the same XFT seed to find any track compatible with the hits found in the corresponding 30° sector (with the sole constraint that all hits belong to the same half-barrel), due to the lack of longitudinal information from XFT. Of course, if occupancy is high, a lot of fake tracks can be generated from the same XFT seed; it could become mandatory to discard these fakes. This can be accomplished by performing a simple linear extrapolation of SVT coordinates to the radius of SL 6: if ϕ_0 and c are angle and curvature measured in the SVT for each track, we can require that no more than one track possesses the same value[10] of

$$\phi_{extr} \sim \phi_0 + 105.575 * c, \tag{1}$$

or, more precisely, the same value of

$$int((\phi_{extr} - 0.625°)/1.25°). \tag{2}$$

Such linear extrapolations are not needed by the Level 2 processors, since the SVT output does include, for each track, the XFT azimuthal measurement received in input[9], which automatically defines track multiplets; we have however verified that the two methods are equivalent.

We obviously need a sound prescription to choose the right track among all the identified candidates fitted using the same XFT seed, if we wish to avoid paying the price of discarding all of them. Our choice is to pick the track with smallest impact parameter: given that fake tracks have a very broad impact parameter distribution (Figs. 6, 9), this choice should select the correct track in most cases, while preserving the discriminating power of those other (single) tracks which are genuinely displaced from the primary vertex.

A comparison of the impact parameter distribution of tracks rescued from a multiplet by the above prescription with the I.P. distribution of the discarded tracks is shown in Fig. 7: indeed, tracks rescued from a multiplet and single tracks exhibit the very same distribution of impact parameter, confirming the soundness of our prescription. Further, Fig. 9 shows that the removal does make a huge difference in the effectiveness of IP-based selections; this can be also verified by comparing Fig. 12 to Fig. 13 (see Subsec. 4.3).

Currently, a custom board ("*Ghostbuster board*") is being designed to select the "right" track in a multiplet without making explicit use of the track's impact parameter.

4.2 Other technicalities

In order to study resolutions, no beam-spot spread in the transverse plane is applied at generation level: all prompt tracks do come from the origin of coordinates, while a 29 cm z-spread is included in the CDF2SIM simulation. For the study of IP-based selections, however, we do need to take into account the effect of a finite beam spot size. This is taken care of by a simple random extraction of a gaussian-distributed radial deviation r_v, of $30 \mu m$ width, and an azimuthal angle ϕ_v, once per event. The effect on track impact parameters is then included by linearly adding to the measured value d the quantity

$$d_v = r_v sin(\phi_t - \phi_v). \tag{3}$$

The effect of this smearing is shown in Fig. 8. As expected, almost no variation is observed in the tails of the distribution, which are the regions we wish to study.

[10] 105.575 is the radius of the center of SL6 in cm, and we adopt a convention according to which curvature is the inverse of the track helix diameter, measured in cm^{-1}.

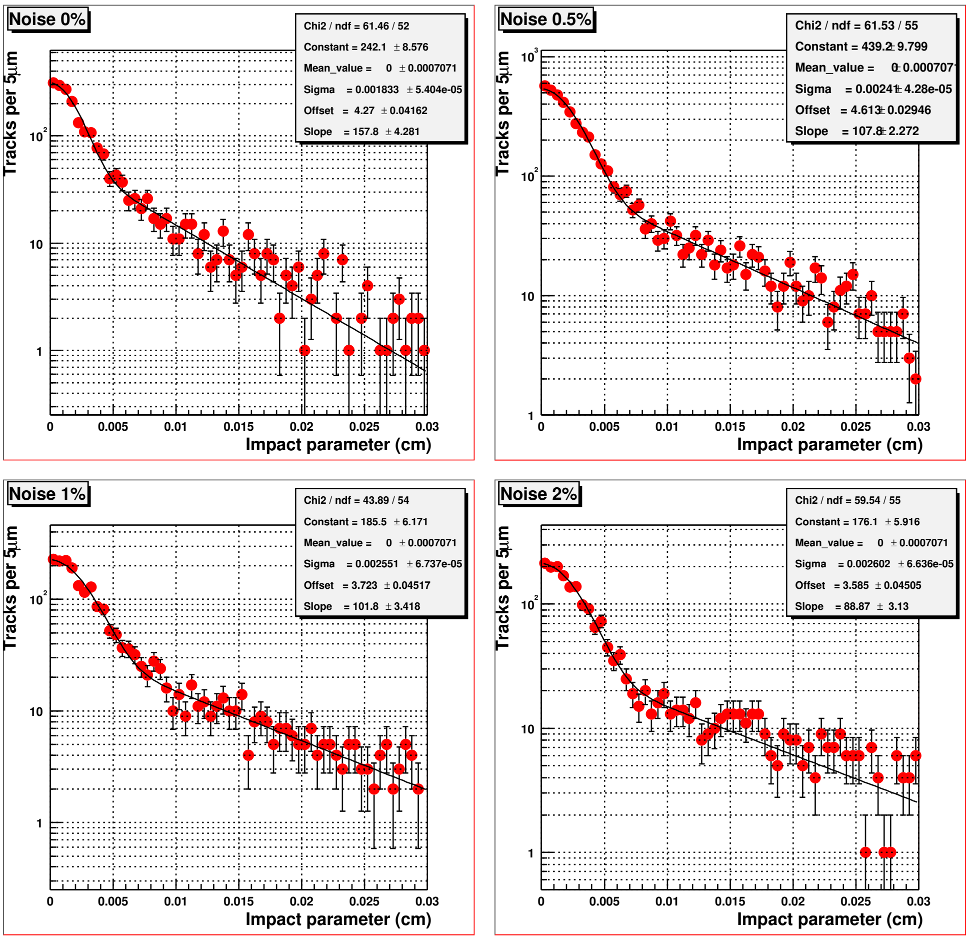

Figure 6: *Impact parameter distributions of SVT tracks in QCD events, for the default χ^2 cut and four different noise levels in the silicon microstrips; the rejection of multiple tracks from the same XFT seed described in Sec. 4.1 is not applied, and no beam spot smearing is operated. Notice the worsening of prompt track IP resolution as the noise level increases. A summary of the impact parameter resolutions fitted from these curves is presented in Fig. 20.*

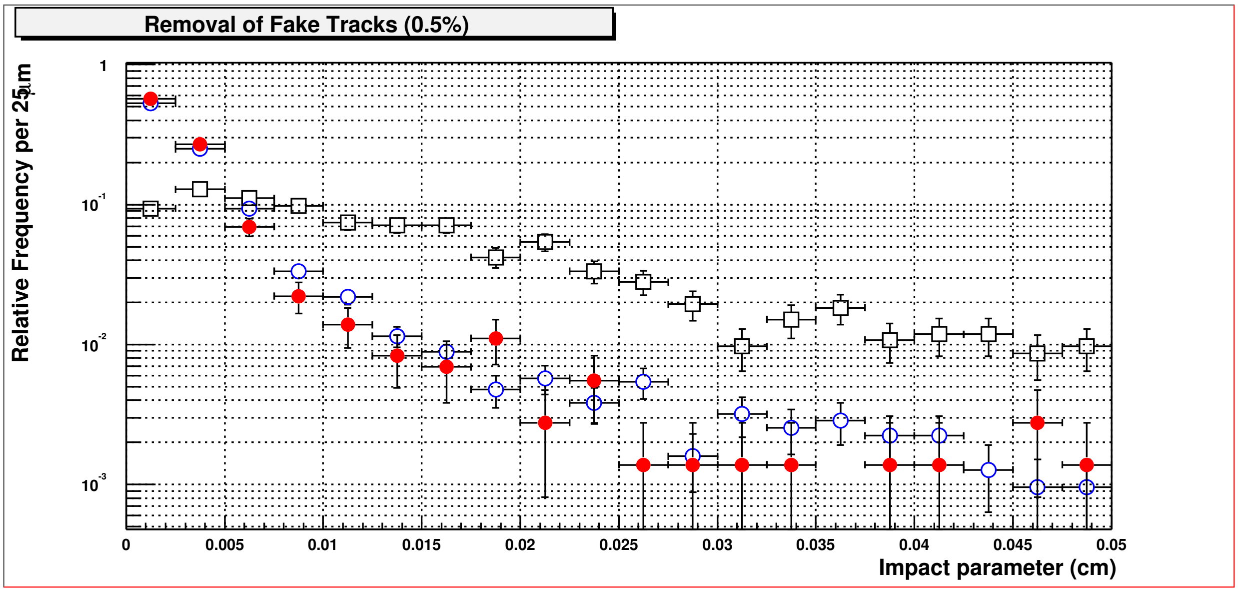

Figure 7: *Impact parameter distributions of SVT tracks belonging to three different categories: tracks univocally associated to an XFT seed (open blue circles), tracks belonging to a multiplet associated to the same seed that have been selected as the right one by the prescription discussed in Sec. 4.1 (full red circles), and tracks belonging to a multiplet that have been discarded by the prescription (open black squares). For this plot, QCD events and a 2% noise level (see Sec. 4.4) have been used; the χ^2 cut was set at its default value; a finite beam spot was simulated as discussed in the text.*

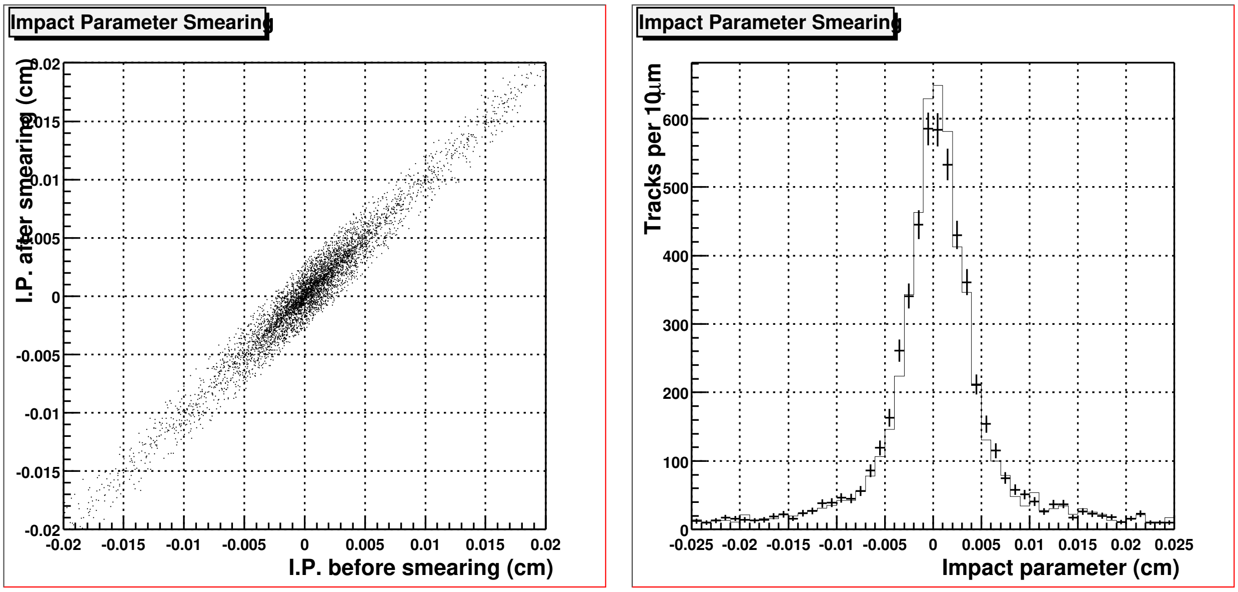

Figure 8: *Effect of the simulation of a finite beam spot size on track impact parameters. Left: impact parameter of tracks before vs after the smearing; right: the same quantities are overlayed. For this plot, QCD events and the default values of noise and χ^2 cut have been used.*

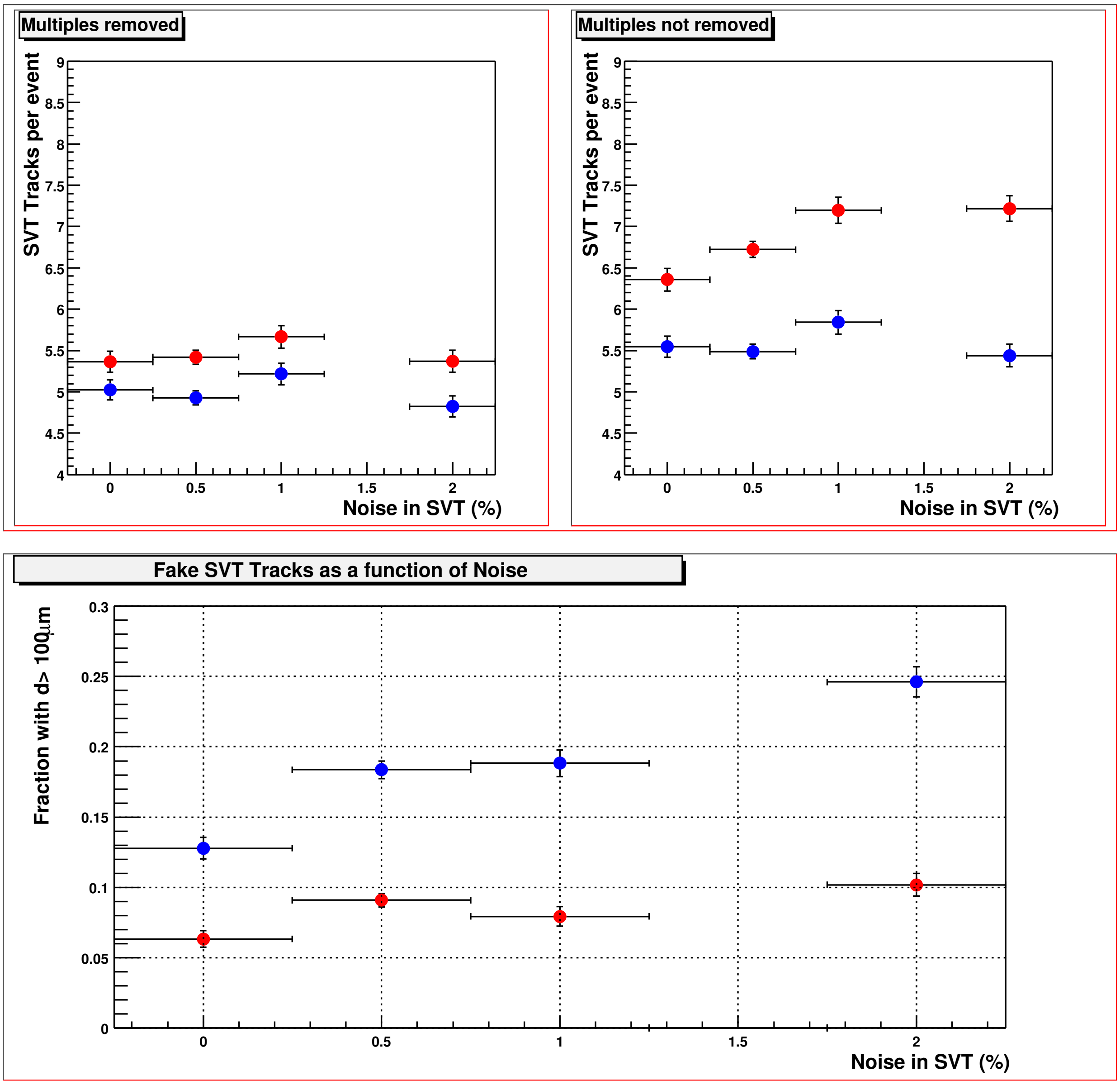

Figure 9: *Average number of SVT tracks as a function of SVX noise with and without multiple track removal. Top left: average number of tracks (red) and tracks with* $|d| < 100\mu m$ *(blue) when the prescription for the removal of multiple tracks is applied. Top right: same when no removal is operated. Bottom: comparison of the fraction of displaced tracks (*$|d| > 100\mu m$*) as a function of noise before (black) and after (magenta) the removal.*

4.3 Optimization of Level 2 Requirements

We wish to determine how much use can be made of the tracking information provided by SVT at Level 2 for the discrimination of $VH \rightarrow 4j$ events from generic 4-jet events produced by QCD processes after calorimetric requirements. The latter are dominated by light quark and gluon jets, and produce tracks that originate from the primary interaction vertex. Their discrimination should therefore be easy in principle, by just requiring that events contain some tracks with significant impact parameter. However, as we have already noted, the SVT has not been proven effective on the very complicated, high-multiplicity and high-P_T tracks that originate from a 4-jet interaction. Its effectiveness must in fact be demonstrated by comparing impact parameter spectra of signal and background events. We expect that the impact parameter distribution in background events will be dominated by prompt tracks peaking at zero, with a small, wide tail due to mismeasured tracks and fake tracks resulting from a random combination of noise hits; real tracks due to early decay of K_s^0 particles will also be contributing to this tail.

All these effects are of course also present in signal events, but how much signal and background distributions differ, and just how many displaced tracks the signal yields (once acceptance, XFT efficiency, and $P_T > 2\ GeV/c$ cut are taken into account), is what we set out to study.

The aim of this study is to find the SVT requirements can lower the rate after calorimetric cuts have been applied, maintaining the efficiency as high as possible. The rate reduction we want to achieve depends on what we are going to do at Level 3. However, we can set 1-1.5 Hz as a reasonable limit for the time being.

We have already shown in Fig. 5 the impact parameter distribution of all tracks with $P_T > 2\ GeV$ reconstructed by SVT and passing the default cut ($\chi^2 < 12.6$) on the fit χ^2 obtained by the simulated track fitter boards, for QCD and HV events. The distributions are indeed different, reflecting the long lifetime of b-quarks from H decay. Ordering these tracks event-by-event by their impact parameter allows to plot the largest and second-largest IP in the event in Fig. 10.

We may perform a simple cut-optimization study on the basis of these and similar other histograms. Defining the signal efficiency $\epsilon_s(x)$ as the number of events where the largest-IP track has $|d|_{max} > x$, and accordingly for the background acceptance $\epsilon_b(x)$, we may compute the shape of the "quality factor"

$$Q(x) = \epsilon_s^2(x)/\epsilon_b(x) \tag{4}$$

(Fig. 11). A simple selection requiring $|d|_{max} > 120\ \mu m$ appears to increase this figure of merit by about 80%, while reducing the background rate by a factor of four. However, if we want to reduce the rate at about 1.0-1.5 Hz, we have to require $|d|_{max} >$ 350-500 μm, with an efficiency of about 35-23% respectively.

In the case of a selection based on the second-largest track IP, $d_{2^{nd}}$, a cut at around 100-150 μm maximizes Q and reduces the rate to the wanted values, with an efficiency of about 50-38% (Fig. 12). This variable appears the most promising for a selection of good events in the sample, since it not only provides the best background reduction, but it also selects events that will very likely allow the reconstruction of one or two displaced secondary vertices, since they possess two very good seed tracks. Fig. 13 points out the importance of

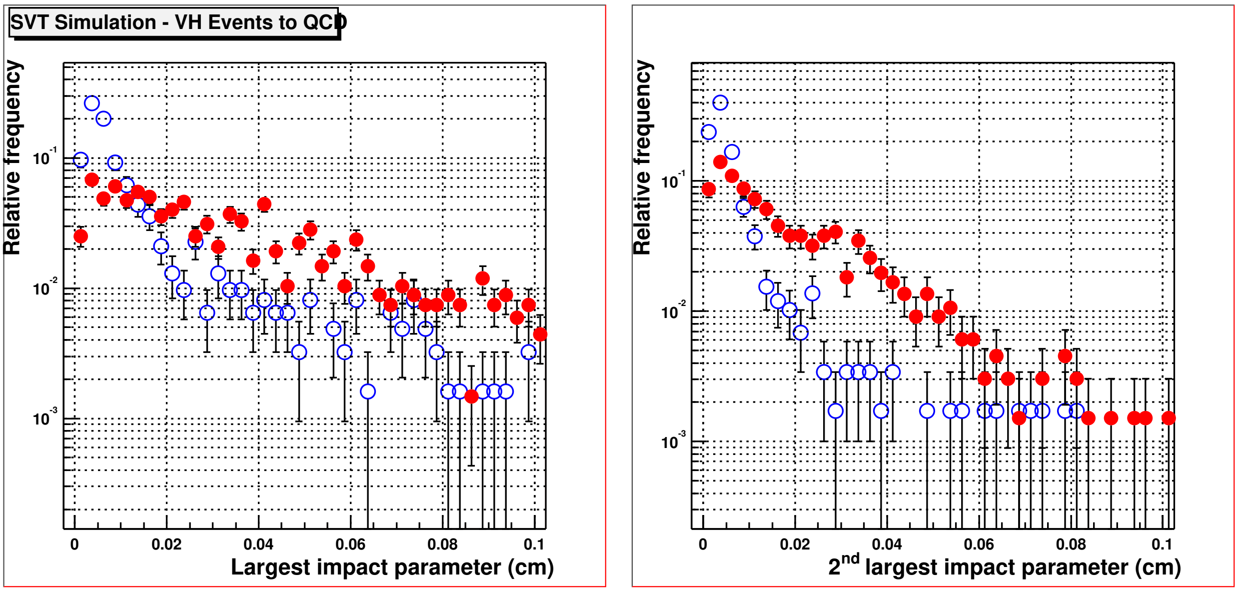

Figure 10: *Distribution of the largest (left) and second-largest (right) impact parameter in VH (open red circles) and QCD events (blue circles). The default values of χ^2 cut and noise level have been used; track impact parameters have been smeared with a finite beam spot size (see Sec. 4.2).*

the multiple SVT tracks removal for this selection: without removal, we find a worsening in the efficiency of about 5-10% at the same rate level.

The high multiplicity of multijet events suggests an examination of the impact parameter of the third track as well. The quality factor Q reaches in that case values close to the ones seen above, but with a lower efficiency (Fig. 14).

Another idea might be that of computing per each event the sum of all impact parameters of those $P_T > 2\ GeV/c$ tracks which have $|d| > 50\ \mu m$, *id est* tracks that appear only marginally consistent (more than 1σ away) with the hypothesis of coming from the primary event vertex (see Fig. 15). Such a selection appears less promising than the ones described above, though, and less straightforward to implement within the strict processing times allotted to the Level 2 processors.

Finally we examine in Fig. 16 the outcome of a hypothetical seletion based on the quadrature sum $N = \sqrt{\sum_i {s_i}^2}$ of impact parameter significance of all SVT tracks in the event, where $s = |d|/0.0025$ is just defined as the impact parameter measured in 25 μm units, with the prescription that $s = 10$ if $|d| \geq 250\ \mu m$. Surprisingly, this approach does not yield better results than the ordinary selection based on $|d_{2^{nd}}|$: a cut $N > 12$ gives a rate of $\sim 1\ Hz$ for a $\sim 40\%$ signal efficiency. These latter exotic approaches may be worth another look only if a significant degradation in impact parameter resolution occurs during data-taking, or in case of other significant changes.

The effect of different Level 1 requirement is investigated in Fig. 17, where the second choise described in the Section 3 is applied. We do not find substantial difference in the SVT performance.

Finally, we have to discuss how the inefficiencies in the simulation of the calorimeter can

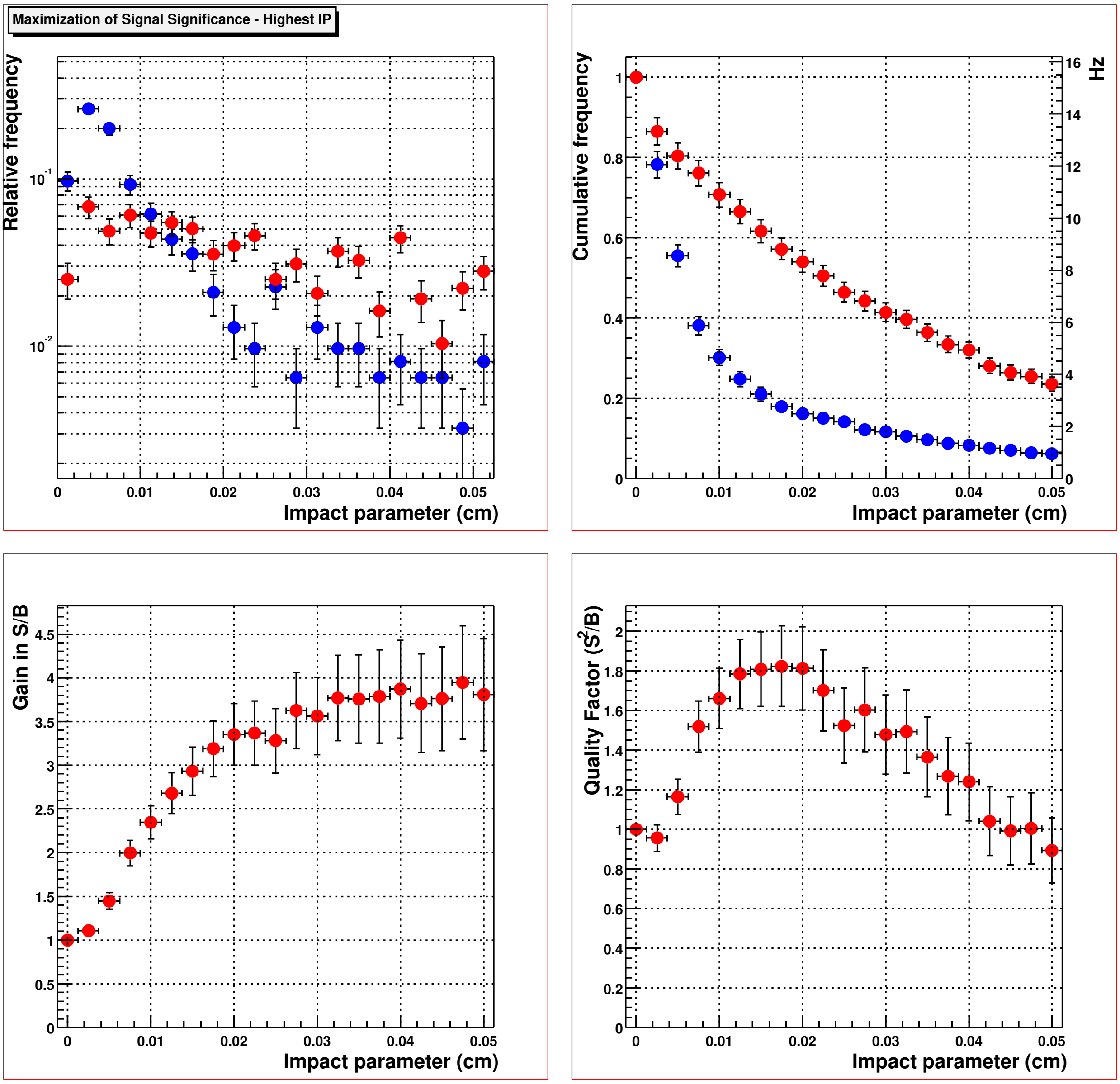

Figure 11: *Optimization of the selection based on the highest-IP track in the event. Top left: highest impact parameter in QCD (blue) and HV (red) events. Top right: efficiency as a function of the cut on the highest IP. Bottom left: ratio between signal and background efficiency. Bottom right: quality factor (see text). The default values of χ^2 cut and noise level have been used.*

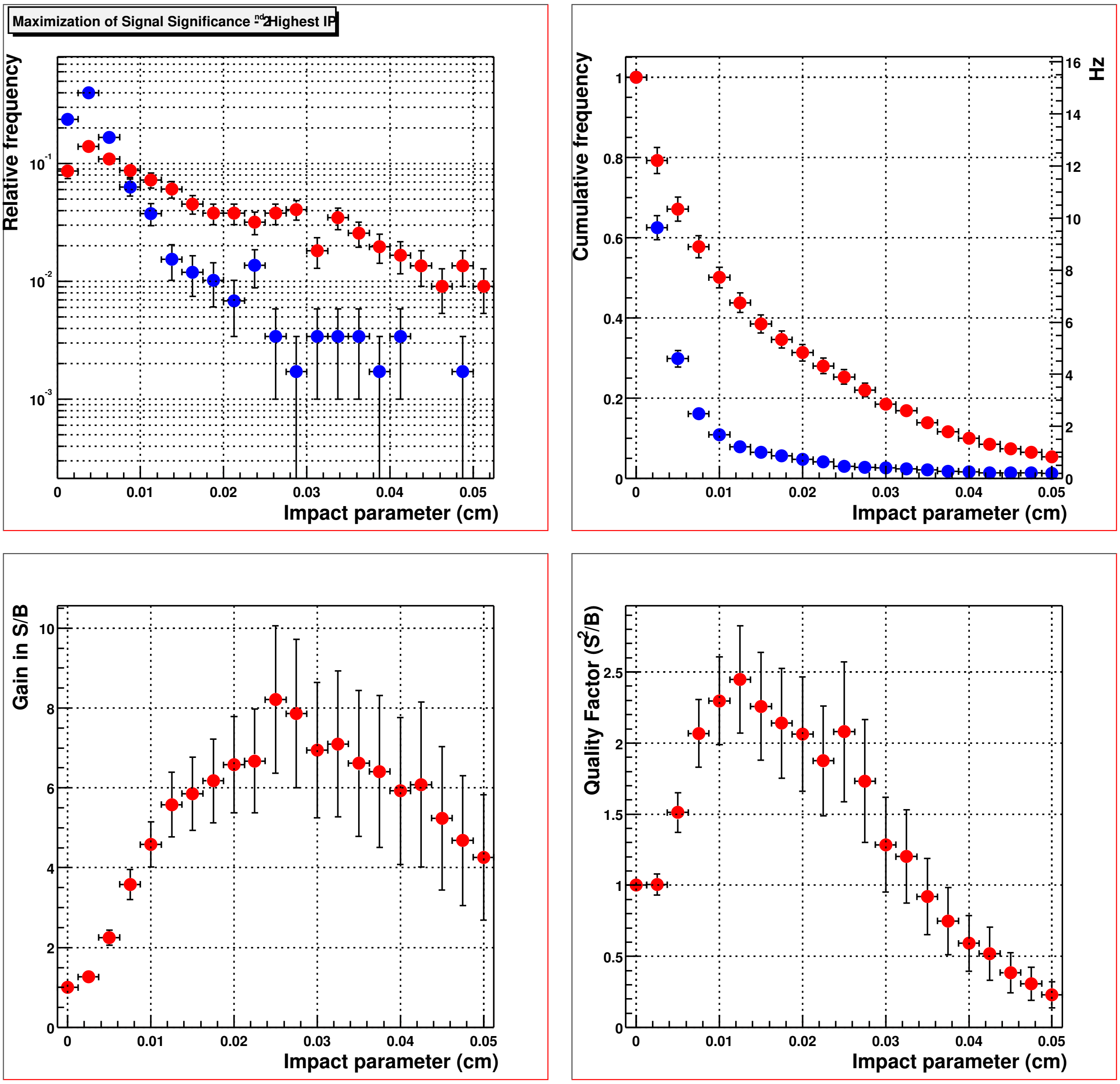

Figure 12: *Optimization of the selection based on the second-highest-IP track in the event. Top left:* 2^{nd}*-highest impact parameter in QCD (blue) and HV (red) events. Top right: efficiency as a function of the cut on the* 2^{nd}*-highest IP. Bottom left: ratio between signal and background efficiency. Bottom right: quality factor (see text). The default values of* χ^2 *cut and noise level have been used.*

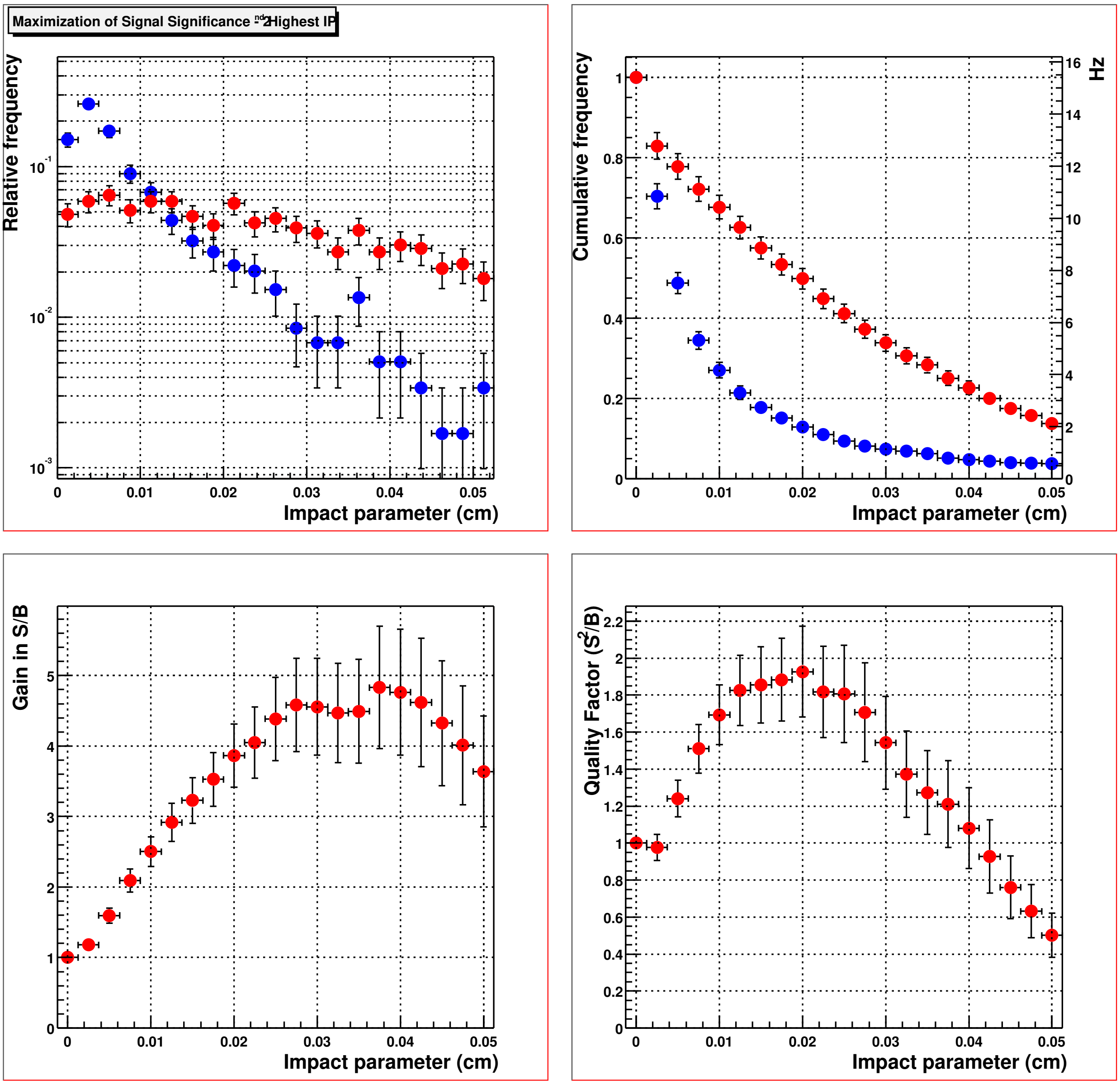

Figure 13: *Optimization of the selection based on the second-highest-IP track in the event, when no removal of multiple SVT tracks extrapolating to the same azimuth on SL6 is performed. Top left: 2^{nd}-highest impact parameter in QCD (blue) and HV (red) events. Top right: efficiency as a function of the cut on the 2^{nd}-highest IP. Bottom left: ratio between signal and background efficiency. Bottom right: quality factor (see text). The default values of χ^2 cut and noise level have been used.*

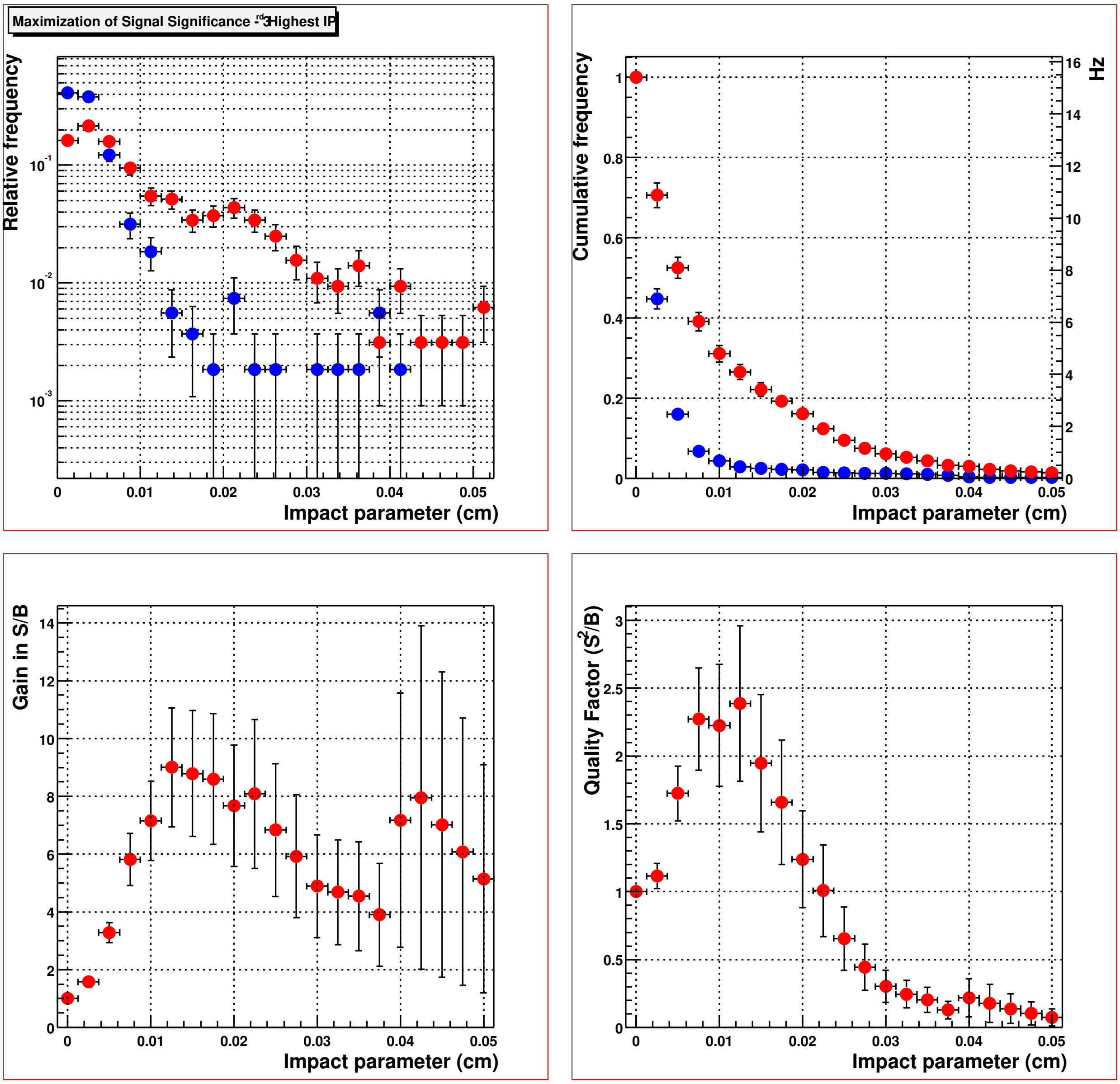

Figure 14: *Optimization of the selection based on the third-highest-IP track in the event. Top left: 3^{rd}-highest impact parameter in QCD (blue) and HV (red) events. Top right: efficiency as a function of the cut on the 3^{rd}-highest I.P.. Bottom left: ratio between signal and background efficiency. Bottom right: quality factor (see text). The default values of χ^2 cut and noise level have been used.*

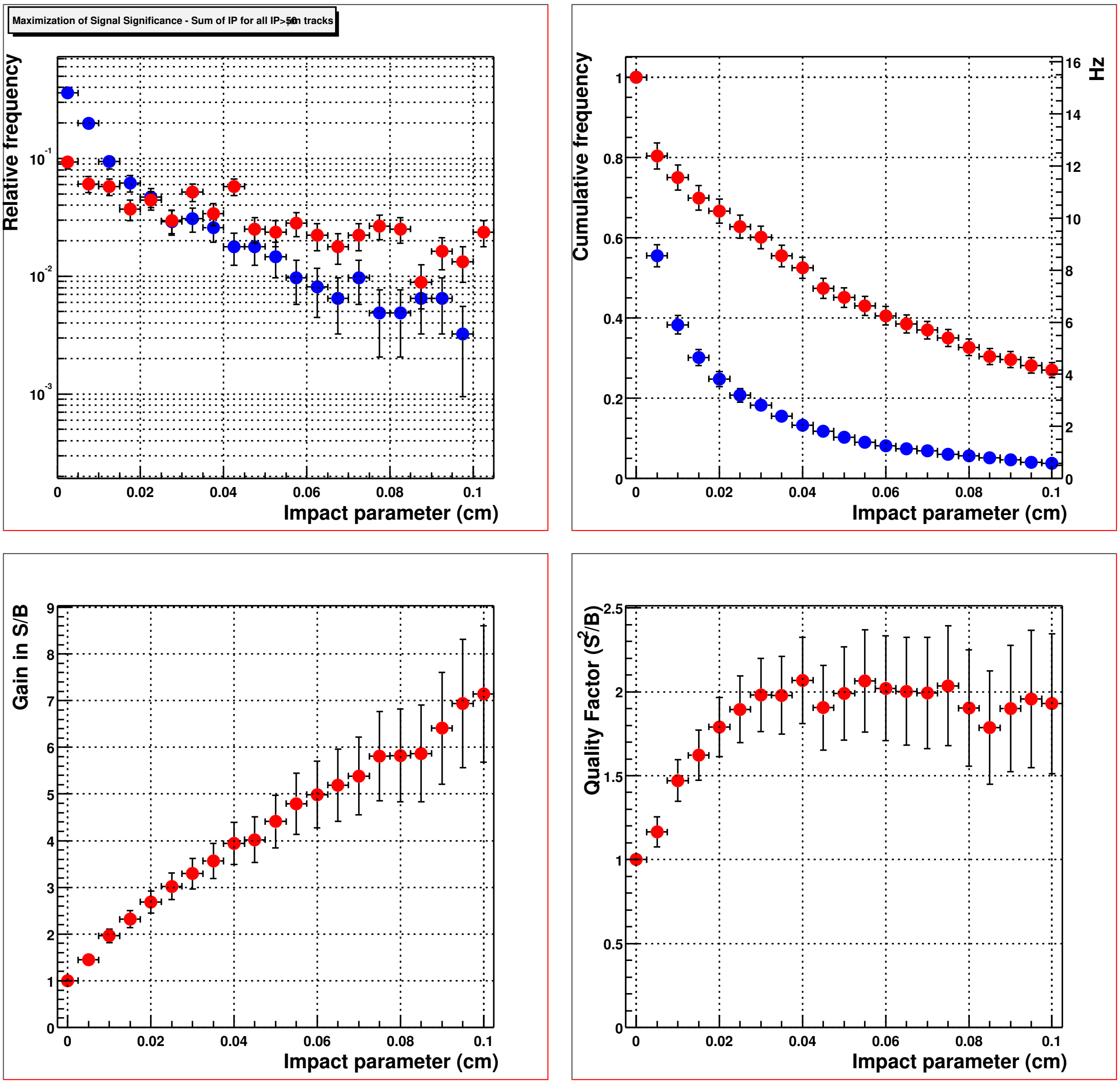

Figure 15: *Optimization of the selection based on the sum of impact parameters of all tracks with* $d > 50$ μm*. Top left: sum of impact parameters in QCD (blue) and HV (red) events. Top right: efficiency as a function of the cut on the sum. Bottom left: ratio between signal and background efficiency. Bottom right: quality factor (see text). The default values of* χ^2 *cut and noise level have been used.*

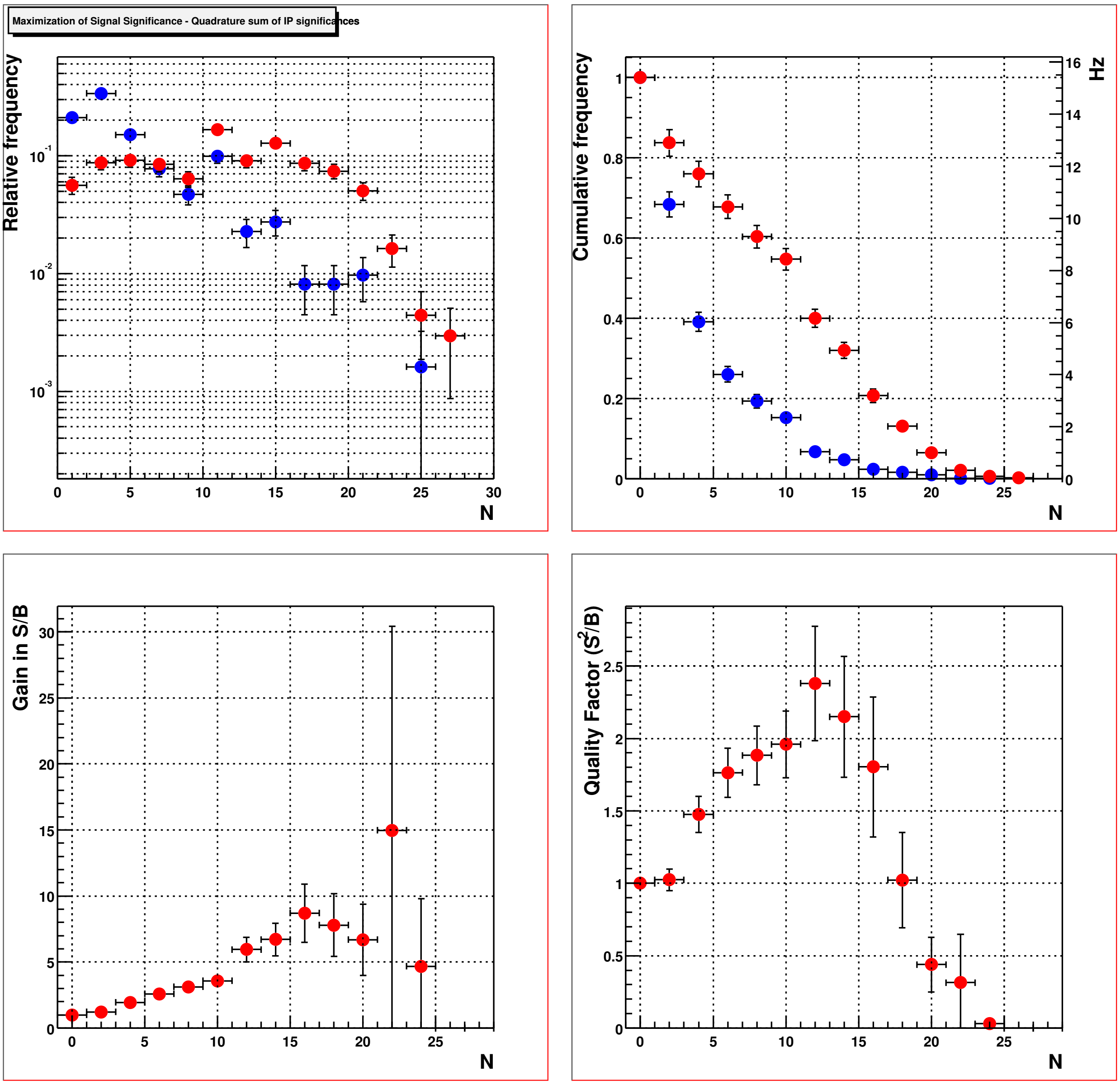

Figure 16: *Optimization of a selection based on the quadrature sum of impact parameter significances of SVT tracks (see text). The quality factor attainable is not larger than those obtained with simpler approaches.*

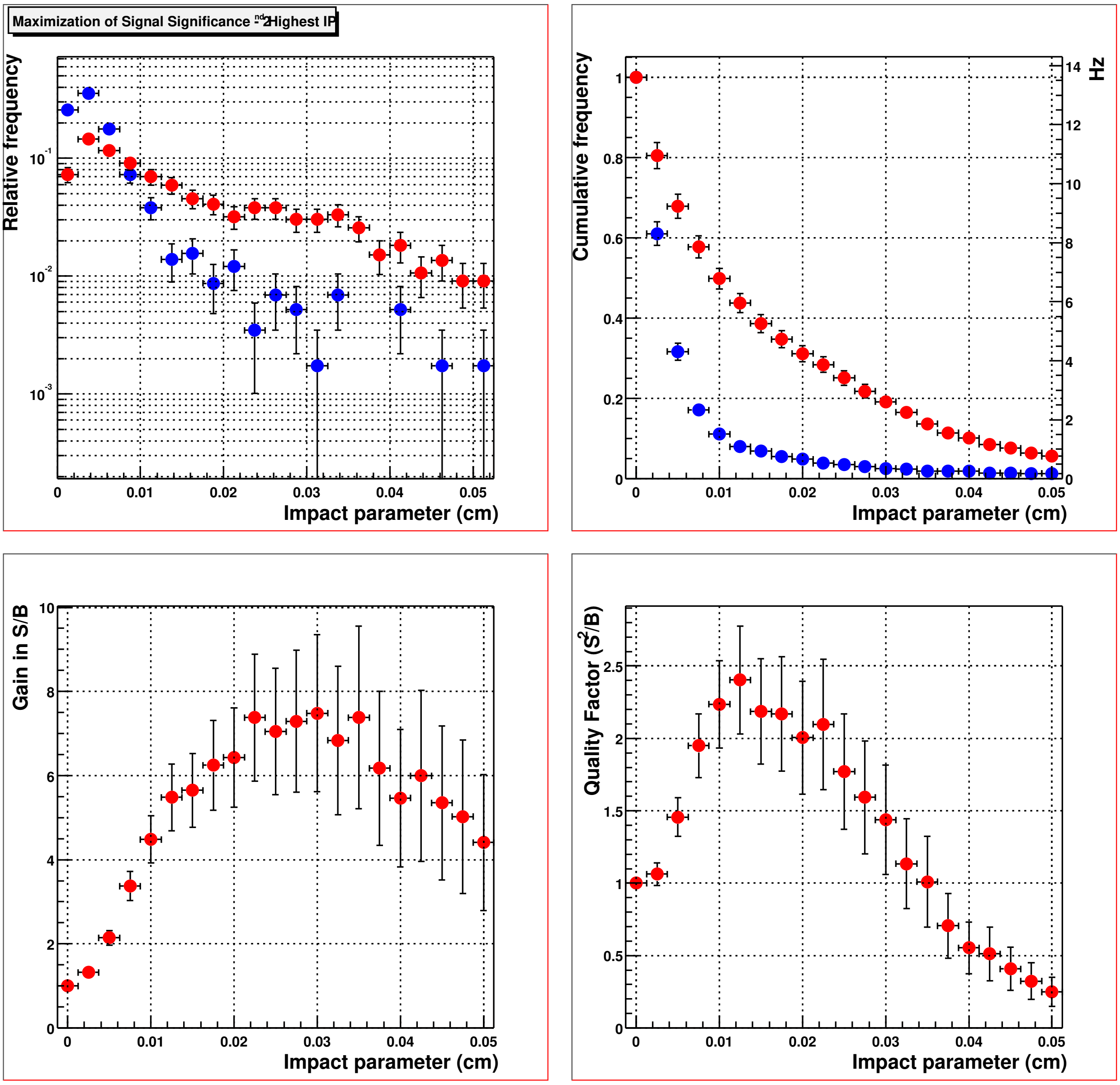

Figure 17: *Optimization of the selection based on the second-highest-IP track in the event, when the second choice for Level 1 requirement is used. Top left:* 2^{nd}*-highest impact parameter in QCD (blue) and HV (red) events. Top right: efficiency as a function of the cut on the* 2^{nd}*-highest IP. Bottom left: ratio between signal and background efficiency. Bottom right: quality factor (see text). The default values of* χ^2 *cut and noise level have been used.*

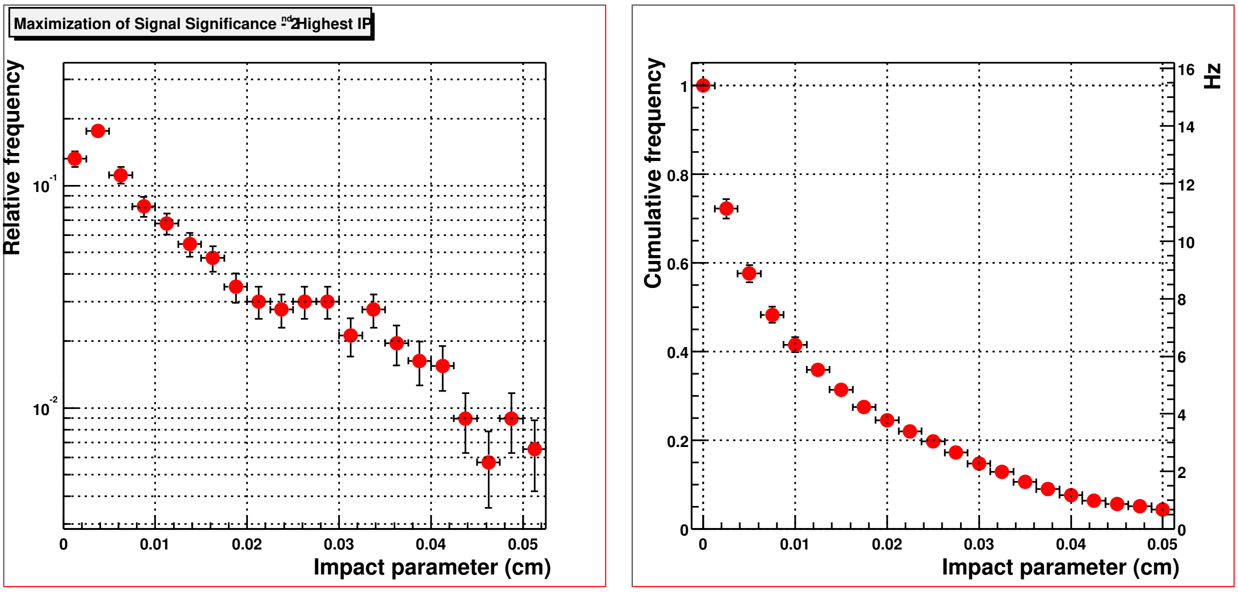

Figure 18: *Efficiency of the selection based on the second-highest-IP track in the event, when no calorimetric trigger is required. Left:* 2^{nd}*-highest impact parameter in HV events. Right: efficiency as a function of the cut on the* 2^{nd}*-highest IP.*

affect these results. We point out in the Section 3 that the calorimetric requirements on our simulation may be something more tightening than on data. Therefore, the rates we estimeted in this Section are probably slightly conservative. As far the efficiency, Fig. 18 shows the effect of a selection based on the second-highest-IP track in the event when no calorimetric cuts are applied: for the cut at around 100-150 μm discussed above, we find a lowering in the efficiency at about $36-42\%$, which can be set as an inferior limit.

4.4 Effect of χ^2 Cut and Noise

4.4.1 Variations with the χ^2 cut

The track fitters in SVT operate a selection of good tracks based on the χ^2 of the fit to hit positions in the four SVX II layers plus the XFT track coordinates. The default cut is typically set to 12.6, a value that corresponds to a $\geq 99\%$ acceptance for real tracks and which appears to suit to events of interest for B physics, where track reconstruction efficiency is critical and occupancy is not very high. Of course, in the much more crowded environment caused by events with four hadronic jets, this cut might be sub-optimal, so we set out to study how efficiency and rate are affected by a change of its value.

We scan seven values of the χ^2 cut for all our simulations: 6, 8, 10, 12.6 (the default value), 15, 20, and 50. For each value of the cut we reprocess the data with the SVT simulation: that allows a comparison of efficiencies and gains as a function of the selections already discussed in the previous section.

Fig. 21 shows how the quality factor changes depending on the choice of χ^2 and IP cut. It is apparent that a stricter cut on the fit χ^2 would improve the discrimination between signal and noise, particularly in the case of a tight impact parameter cut (see Fig.19). However, the effect around the critical range if the rate (1-1.5 Hz) is not very large, so that a tighter χ^2 cut appears a useful option only if background rates become a critical issue.

The same study can be repeated for the various level of noise in the silicon strips, yielding similar results: in all cases, a tighter χ^2 has been found to slightly improve background rejection (see Fig. 22 for the case of 2.0% of noisy strips).

4.4.2 Variations with the noise level

In a given silicon strip on average a real signal from a minimum ionizing particle amounts to roughly 20,000 electrons, equivalent to about 30 ADC counts. The average amount of electronic noise varies half-ladder by half-ladder throughout the detector but is seldom larger than a few ADC counts; the readout thresholds to suppress it have been set to $2.5 - 3.0$ standard deviations of its value. However, noisy strips exist in all ladders of the detector, and they may have a definite impact in the performance of the SVT, particularly for the crowded topology we are focusing on here. It is necessary to note that the superstrip size chosen for this simulation (300 μm) implies that even a 2% of noisy strips amounts to 9.6% of fake single-strip hits in input to SVT, a number that is already able to confuse the track-hit matching with a certain frequency (see Fig. 20). Moreover, it has been shown[10] that noise in the inner layers is particularly bad for impact parameter reconstruction, because an accidental hit chosen by the AM in layer 0 in place of the real one will significantly degrade the I.P. resolution σ_d; however, even when the electronic noise does not cause the identification of an independent fake hit, it can worsen appreciably the resolution.

The fraction of noisy and dead silicon strips in the silicon layers has been measured and is known in detail in each of the 360 half-ladders that constitute the SVX II detector. In principle, one could use the map of noisy and dead channels for a detailed simulation of the SVX II output in the study of the SVT response; however, the information is only available in the form of an Excel spreadsheet at the time of writing, and the task of converting it to

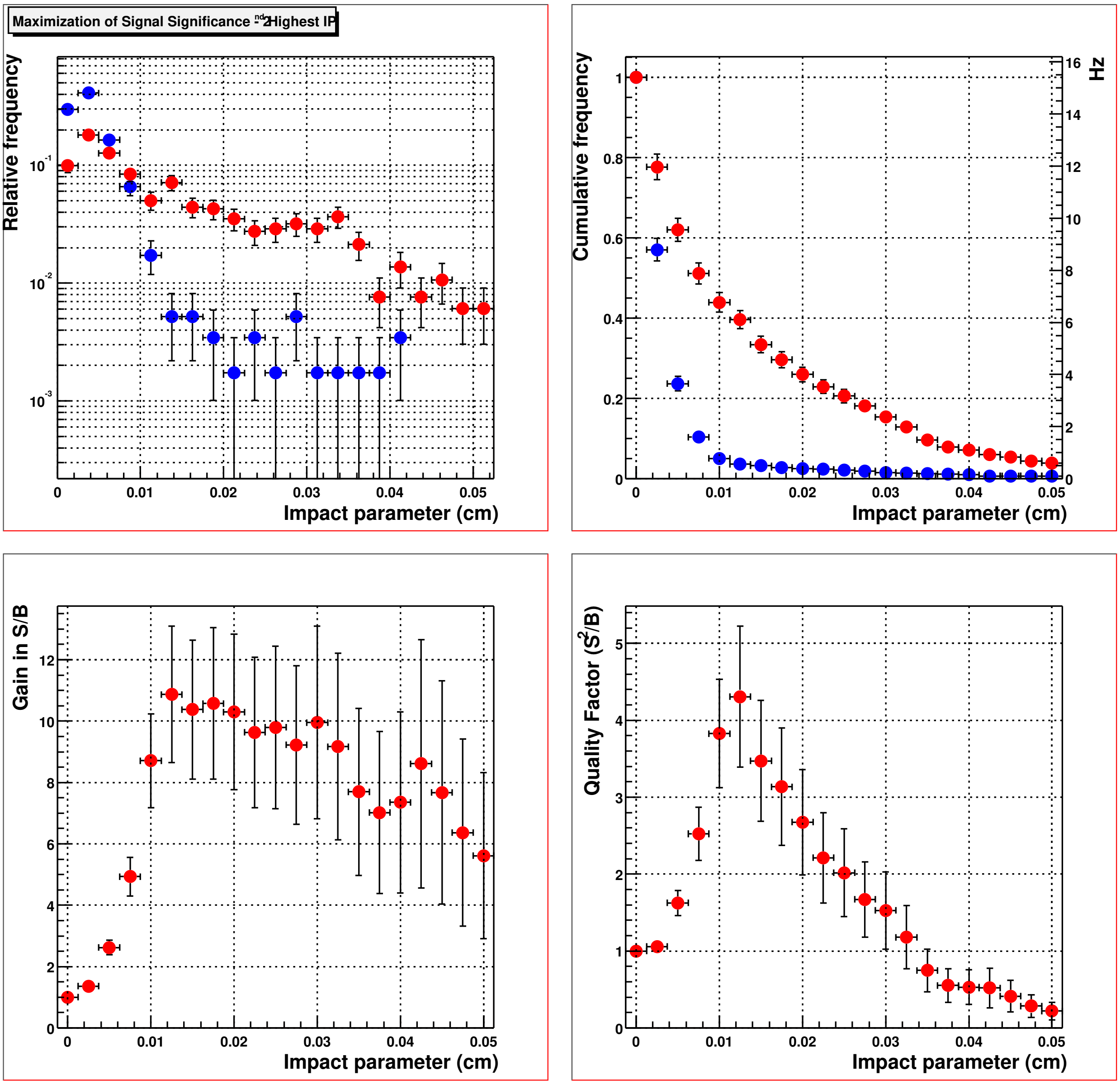

Figure 19: *Optimization of the selection based on the second-highest-IP track in the event, for tracks selected by SVT with a* χ^2 *cut at 8. Top left:* 2^{nd}*-highest impact parameter in QCD (blue) and HV (red) events. Top right: efficiency as a function of the cut on the* 2^{nd}*-highest IP. Bottom left: ratio between signal and background efficiency. Bottom right: quality factor (see text). The default value of noise level has been used.*

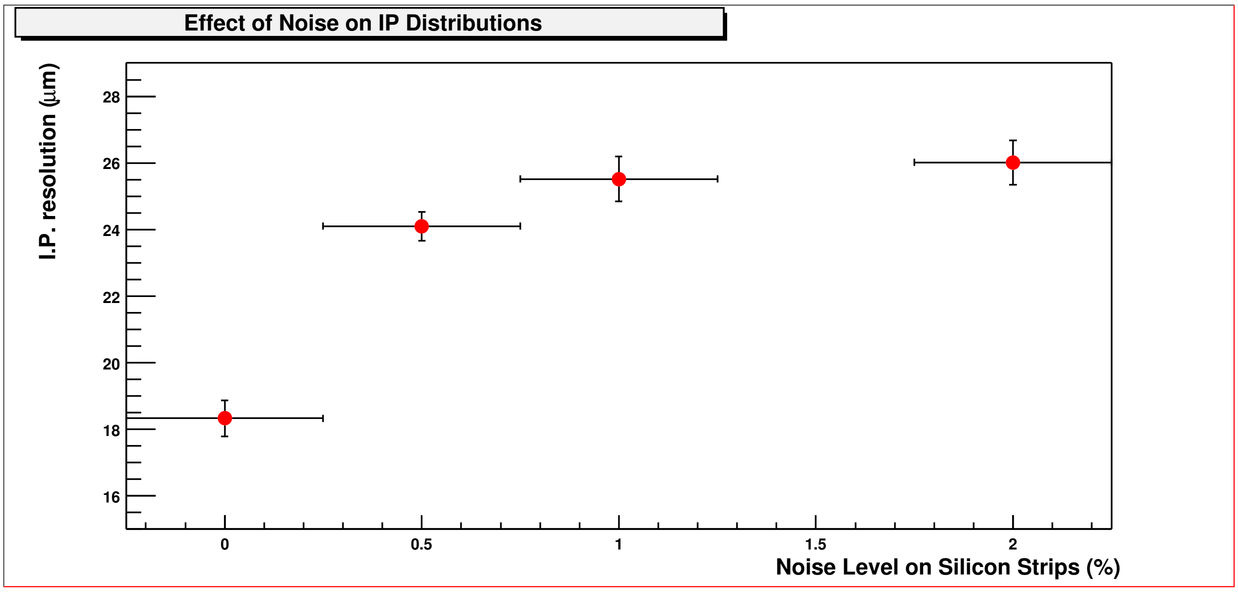

Figure 20: *Impact parameter resolution of prompt tracks reconstructed by SVT as a function of the noise level in the silicon. QCD events have been used (see the fits in Fig. 6).*

a format suitable for consumption by GEANT3 has not been undertaken. We rather use a uniform value of noise in the detector. A random amount of electronic noise is generated by adding ADC counts to the strips, such that a given fraction of them surpasses the readout threshold. We set this fraction at 0.0%, 0.5%, 1.0% and 2.0% to study how it affects the number of reconstructed tracks, the resolution of the track parameters, and the signal efficiency and background rejection. The 0.5% figure should be close to the situation of our real detector[11]. As noted above, this noise does not only affect SVX II occupancy, but also the resolution in the position measurement for multiple-strip clusters caused by real particles, since the smearing affects the computed cluster centroid.

We have measured the impact of the noise level by comparing efficiency and acceptance of each considered selection strategy for the four considered percentages of noisy strips. A performance degradation is observed in all cases with the increase of noise level: the acceptance for background events increases much more rapidly than that of the signal.
In the case of a straightforward selection requiring two displaced tracks with $|d| > 100\ \mu m$, signal acceptance remains approximately constant when the fraction of noisy strip goes from zero to 2%, in the face of a doubling of the background, from 6 (correspondent to $\sim 0.9\ Hz$) to 13% (correspondent to $\sim 2\ Hz$); the quality factor thus decreases considerably (see Fig. 23). A noise level of 2% or larger would decrease the utility of SVT in the discrimination of heavy flavors in the 4-jet data sample; however, in that case a smaller superstrip size -if applicable- could probably restore the discrimination power.

[11] G. Bolla, private communication.

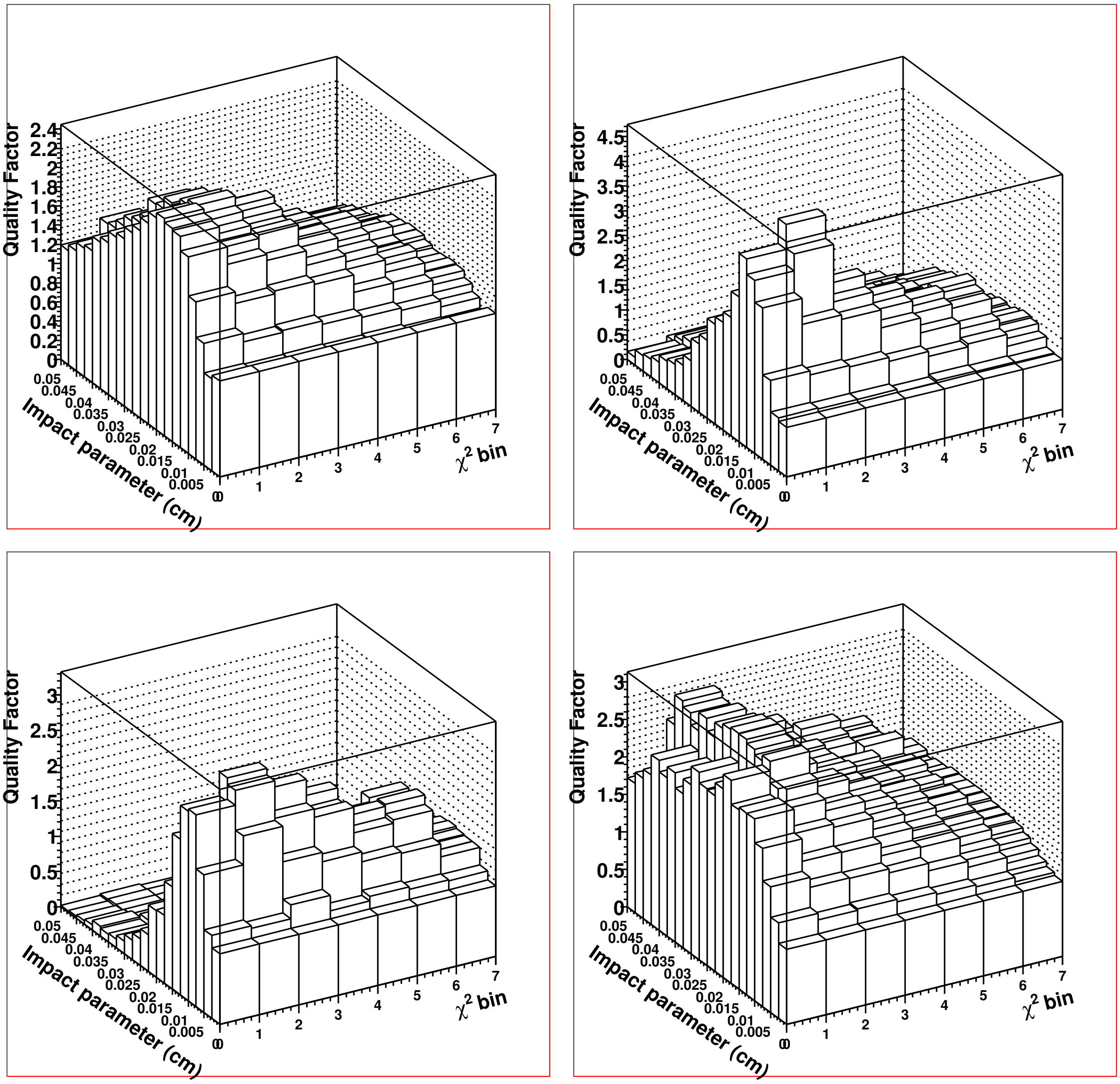

Figure 21: *Variation of quality factor with the choice of the* χ^2 *cut on SVT tracks. Bins 1 to 7 in the abscissa denote cuts at 6, 8, 10, 12.6, 15, 20 and 50, respectively. Top left: quality factor for a selection based on the impact parameter of the highest-IP track. Top right: Q values for a selection based on the impact parameter of the second-highest-IP track. Bottom left: Q values for a selection based on the impact parameter of the* 2^{nd}*-highest-IP track for events having at least one track with* $|d| > 100\ \mu m$*. Bottom right: Q values for a selection based on the sum of impact parameters of all tracks with* $|d| > 50\ \mu m$*. The default value of noise (0.5%) has been used for all plots.*

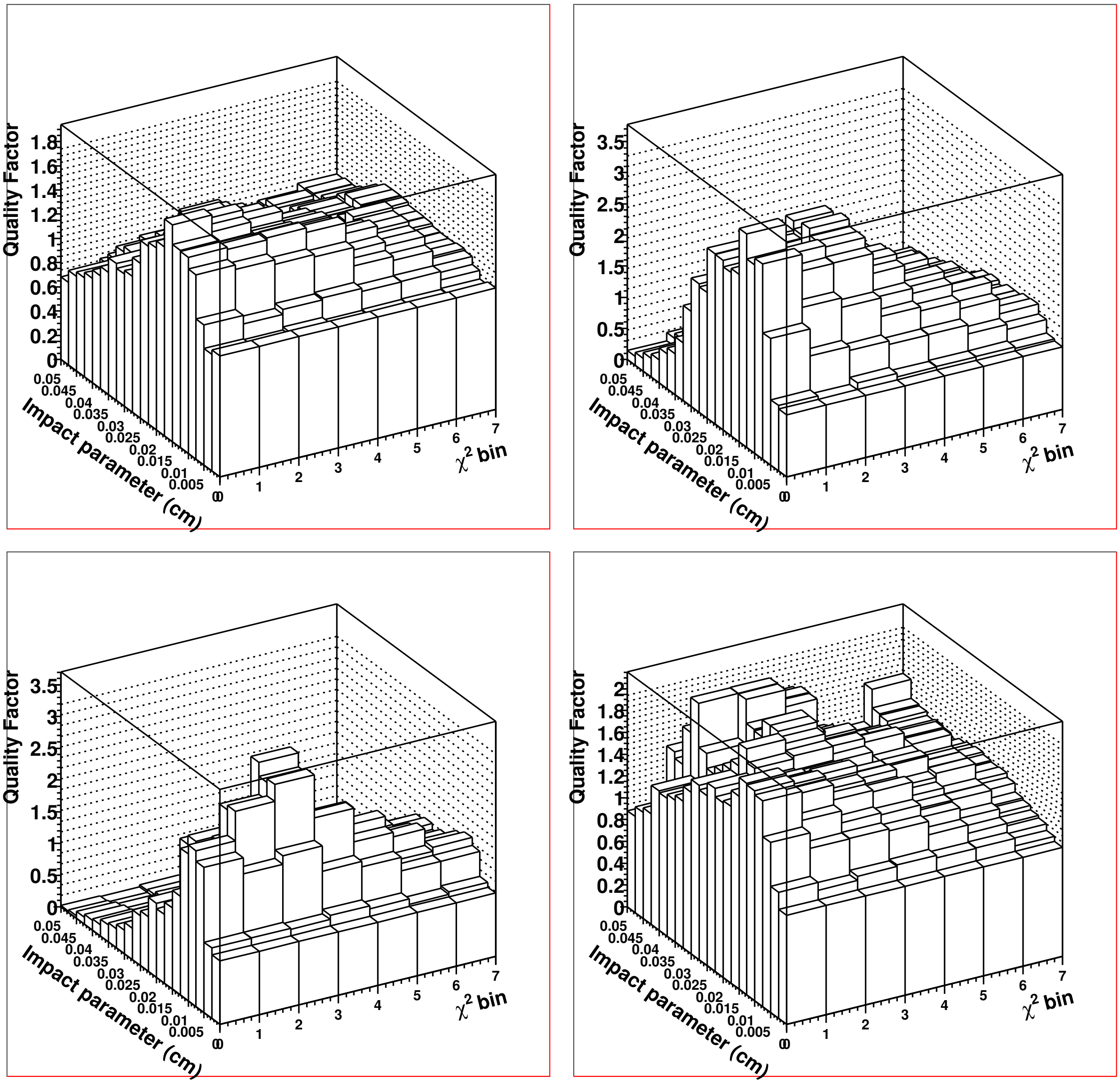

Figure 22: *Variation of quality factor with the choice of the χ^2 cut on SVT tracks. Bins 1 to 7 in the abscissa denote cuts at 6, 8, 10, 12.6, 15, 20 and 50, respectively. Top left: quality factor for a selection based on the impact parameter of the highest-IP track. Top right: Q values for a selection based on the impact parameter of the second-highest-IP track. Bottom left: Q values for a selection based on the impact parameter of the 2^{nd}-highest-IP track for events having at least one track with $|d| > 100$ μm. Bottom right: Q values for a selection based on the sum of impact parameters of all tracks with $|d| > 50$ μm. The highest value of noise (2.0%) has been used for all plots.*

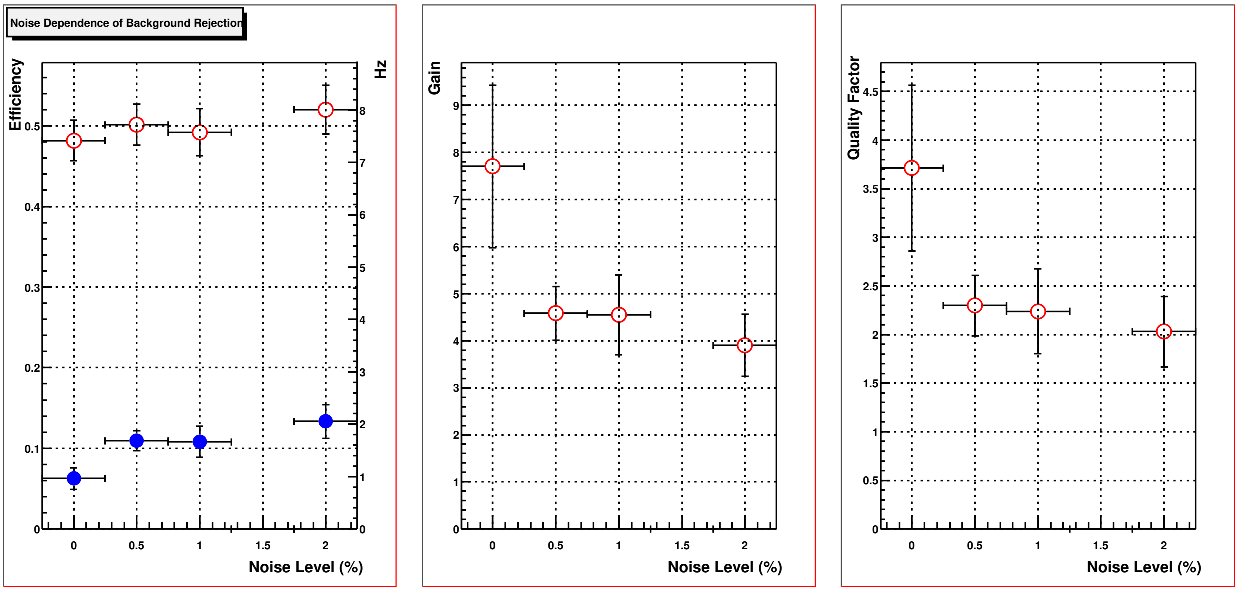

Figure 23: *Degradation of the effectiveness of a selection based on the 2^{nd}-largest impact parameter in VH events ($|d_{2nd}| > 100\ \mu m$) with the noise level in the silicon strips. Left: signal efficiency (red) and background acceptance (blue); center: gain of the selection (S/N); right: quality factor.*

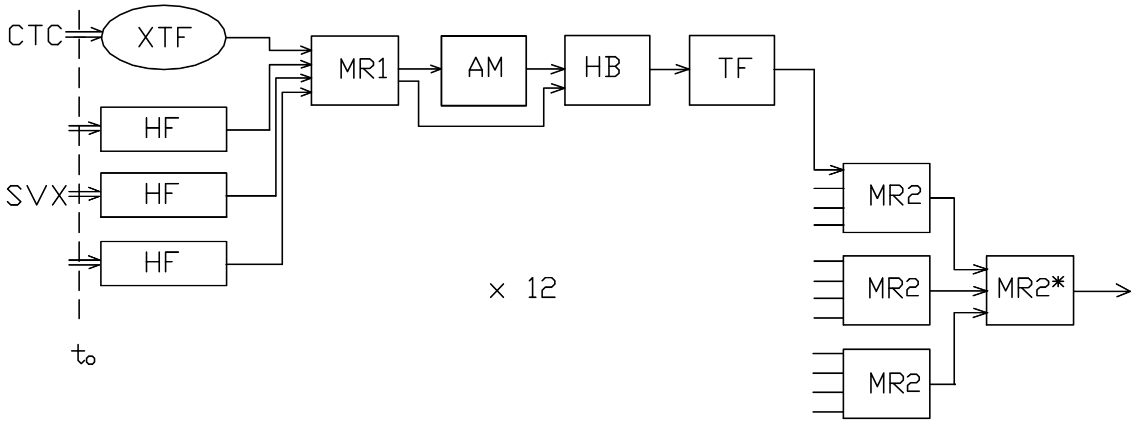

Figure 24: *A schematic view of the block model of the SVT system used for timing estimates (from Ref. [11]).*

4.5 Timing Issues

Timing is critical at trigger Level 2. On average, in a matter of less than 20 microseconds from Level 1 accept the raw data from the detector components has to be analyzed, such that the Level 2 processors can decide whether to pass the event to Level 3. The SVT has been shown to be able to achieve that aim well within the allotted time with the typical events interesting for B-physics issues[11], using a simple timing model. We reproduce that study here for the more complicated $VH \rightarrow 4j$ and possible background events we are interested in.

As said in Sec. 3, we want to consider the possibility of choosing between two different Level 1 calorimetric requirements in order to select the signal events. The first, referred to as *single tower trigger* in the following, takes in exam events which have a single calorimetric tower with total transverse energy, i.e. electromagnetic plus hadronic energies, over 10 GeV. The latter, the *double tower trigger*, selects events with 2 XFT tracks with p_T over 2 GeV/c and two central calorimetric towers with $E_{em} + E_{had} \geq 2\ GeV$. For more details see [7].

4.5.1 The timing model

A clear and detailed description of the timing model devised by G. Punzi, G. Chlachidze and V. Glagolev is given in Ref. [11]. Here we just summarize it briefly in order to set the stage for the discussion of our specific case.

The SVT system can be thought as a set of 12 parallel data streams, each composed of a few functional blocks connected by cables. Blocks identify the hit finders (HF), the first mergers (MR1), the associative memory boards (AM), the hit buffers (HB), the track fitters (TF), and the final mergers (MR2). Each block receives data relative to a single 30° slice of SVX II[12], processes it, and distributes it to one or more blocks downstream. The final information is then merged and output to the Level 2 processors in the form of a track list (see Fig. 24).

[12]That is, data from all ladders at the same ϕ.

For timing estimations, one can model the data flow through each block with a few constants (partly measured on real prototypes and partly estimated with simulations) which describe the cable delay, the processing time, and the time required to input and output each data word. We adopt here the terminology of Ref. [11], where t_1^{in}, t_1^{out}, t_2^{in}, and t_2^{out} are the times when the first (1) or last (2) dataword appears in input or output to each block. Given the constants per each block, the total SVT processing time (t_2^{out} for the last block in the chain) can be then estimated using the number of datawords flowing through each block. To those numbers one should add a 1.5 to 2.0 μs delay from Level 1 accept, to account for the digitization of the data.

4.5.2 Processing time for multijet events

As before, we consider as our default data the simulation with 0.5% of noisy SVX II strips. The distribution of total processing time for VH events in the four jet final state is shown in Fig. 25, while a breakdown of the individual contribution of each functional block is presented in Fig. 26 and in Table 1. Because of the 12-fold parallel architecture of the considered model, the delays introduced by the blocks do not add up to the total processing time; instead, one may define each block's delay as

$$\Delta t_i = max_{j=1}^{12}(t_2^{out})_{i,j} - max_{j=1}^{12}(t_2^{out})_{i-1,j} \tag{5}$$

where j runs on the twelve $30°$ slices, and i denotes the considered block. Thus defined, the individual delays will add up to the total processing time.

From a first inspection of the plots, one notices that the bulk of the events take less than 20 microseconds to be processed, but a significant fraction exceeds that value considerably. The blocks most responsible for the long processing time are the track fitters, although hit buffers also take a relatively long time to process the data; the latter are also more sensitive to the number of reconstructed hits.

A more detailed look at the individual contributions to the processing time for signal can be illustrated by Fig. 27 and for background by Fig. 28 . Here the average value of the t_1^{in}, t_2^{out}, $min(t_1^{in})$, and $max(t_2^{out})$ values are presented for each block in cascade, to highlight the effects of parallelism.

Given the long tails of the total SVT processing time for $VH \to 4j$ events, a number of special interest for the Level 2 trigger is the time necessary to process a given fraction of the considered events. Fig. 29, Fig. 30 and Table 2 and 3 show the time after which 85%, 90%, 95%, and 99% of the events of signal and background have been output by SVT with two different calorimetric triggers used. It appears obvious that a $20 \sim 30 \mu s$ cutoff by the Level 2 processors would significantly hinder the collection of this category of events; on the other hand, the overhead in dead time caused by a delayed Level 2 decision appears small, given the relatively small rate of this kind of events[13]. A more sophisticated analysis,

[13]During Run I the single tower trigger designed for the hadronic top search, which required four jets with $E_T > 15$ GeV and a total $\sum E_T > 125$ GeV, and collected events with characteristics quite similar to the VH events discussed in the present study, had a Level 2 cross section of about 4 nb. An upper limit on the rate of time-intensive events such as the ones discussed here can be inferred from the estimated Level 2 cross section of a trigger recently proposed for collecting VH decays in the single tower channel, which relies

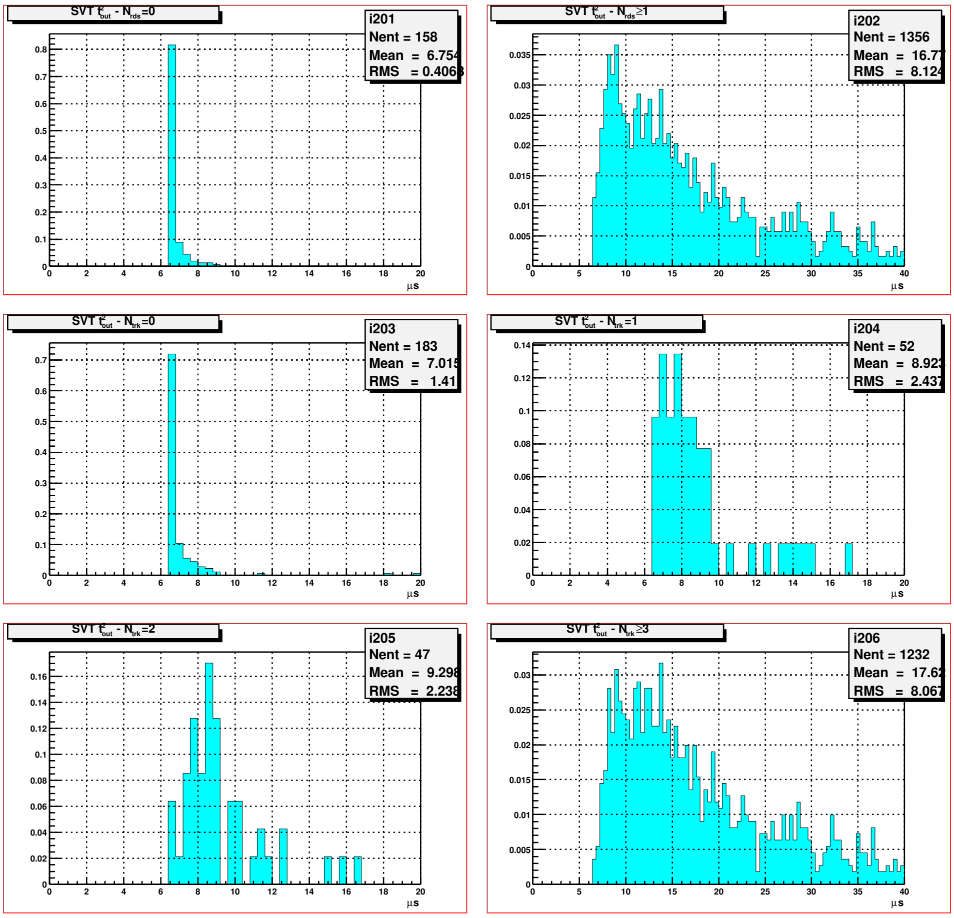

Figure 25: *Total processing time for different categories of SVT output. Top row: events with no found roads (left); events with at least one found road (right). Middle row: events with zero found SVT track (left); events with one found track (right). Bottom row: events with two found SVT tracks (left); events with three or more found tracks (right). The default value of noise level and single tower trigger have been used.*

taking into account several different classes of events, would be required for an estimate of the dead time introduced by a non-time-limited SVT output. We believe this will be better accomplished once we start collecting data.

4.5.3 Dependence on the noise level

As already noted, the processing time of some of SVT's functional blocks depends strictly on the number of hits reconstructed from strips above ADC threshold, while for others the dependence is only indirect, through the increased number of roads and tracks that can be reconstructed. The clearest example is given by the time needed by the MR1 and MR2 blocks: the processing time of the former depends linearly on the number of hits,

on a SLT requirement at Level 3 to increase the heavy flavor content. This trigger would require just three $E_T > 10\ GeV$ jets and a cluster $\sum E_T > 90\ GeV$ at Level 2, with a cross section of the order of 150 nb[5].

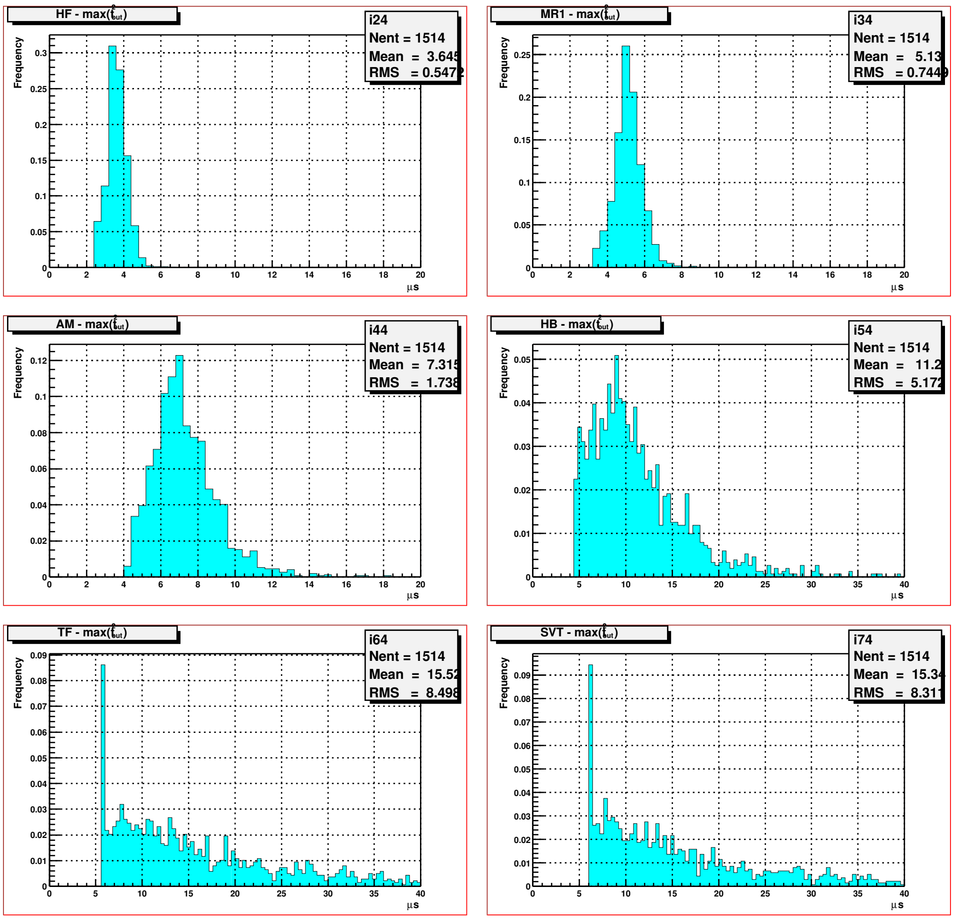

Figure 26: *Cumulative processing time of each SVT functional block for $VH \rightarrow 4j$ events. The default value of noise level and single tower trigger has been used.*

Data sample	HF (μs)	MR1 (μs)	AM (μs)	HB (μs)	TF (μs)	MR2 (μs)	MR2* (μs)	SVT (μs)
VH ($M_H = 120\ GeV$)	3.64	1.50	2.18	3.93	7.68	0.36	0.29	18.87
B-20 (Ref. [11])	3.52	2.56	1.45	1.51	1.74	0.30	0.30	11.39
B-10 (Ref. [11])	3.31	2.44	1.15	0.67	0.92	0.30	0.30	9.06

Table 1: *Average processing time of each SVT functional block for different datasets: 4-jet decays of WH and ZH events for $M_H = 120\ GeV$ and $M_H = 80\ GeV$ with lifetimes turned off, and B production simulations at $P_T^{min} = 10\ GeV$ and $20\ GeV$ from Ref. [11]. Note: noise in the silicon strips was generated differently in the studies of Ref. [11]; therefore, the values most dependent on the total number of hits in the silicon strips (MR1 in particular) do not warrant a direct comparison. However see below for a description of noise effects on the timing.*

and it increases by an order of magnitude as the noise level increases from 0% to 2%; the processing time of the latter is basically a constant, being dominated by its internal delay.

Fig. 31 affects the average processing time of each block for VH events; the individual numbers for the signal are provided in Table 2 for the background in Table 3.

We should note that the level of noisy strips in the SVX II strongly affects the processing time for background events, taking it near to the critical threshold of 20-30 μs. It would be very important to keep under control this variable during the collection of data.

Given the trigger rate for Level 1, of 2.7 kHz, and given that with the 0.5% of noisy strips, the maximum time to process background events is less that 8 μs, we infer that SVT would the busy for about 2.0 % of its time to process this kind of events.

$VH \to 4jets$	HF (μs)	MR1 (μs)	AM (μs)	HB (μs)	TF (μs)	MR2 (μs)	SVT (μs)
0.0%	2.89	0.47	1.98	2.87	4.85	0.12	13.25
0.5%	3.64	1.50	2.18	3.93	7.68	0.36	18.87
1.0%	4.33	2.65	2.36	5.11	8.57	0.34	23.00
2.0%	5.66	4.90	2.75	7.42	10.45	0.50	31.00

Table 2: *Average processing time of each SVT functional block for 4-jet decays of* WH *and* ZH *events (*M_H = 120 GeV/c^2*), for the four different noise levels. Single Tower trigger has been used. See also Fig. 31.*

Background	HF (μs)	MR1 (μs)	AM (μs)	HB (μs)	TF (μs)	MR2 (μs)	SVT (μs)
0.0%	2.55	0.33	1.18	0.60	1.18	0.21	6.37
0.5%	2.11	1.26	1.15	0.76	1.08	0.17	7.85
1.0%	3.79	2.42	1.16	1.34	1.18	0.20	10.41
2.0%	5.16	4.68	1.25	2.85	1.53	0.10	15.88

Table 3: *Average processing time of each SVT functional block for QCD background events for the four different noise levels. Single Tower trigger has been used.*

4.5.4 Dependence on the calorimetric trigger used

We repeat with the double tower trigger the timing studies we have illustrated in the previous subsections for the single tower trigger. Table 4 and Table 5 contain all information about the time to process 85% 90% 95% and 99% of the events respectively for the two possible choices.

The processing time of a given fraction of events, of signal or of background, generally only increases by less than 1 μs passing from the single tower trigger to the double tower one. So, as plots and tables show, there is not a strong dependence in our timing results on the choice of Level 1 requirements. See Fig. 32 and Fig. 33.

SINGLE TOWER TRIGGER	t(85%) (μs)	t(90%) (μs)	t(95%) (μs)	t(99%) (μs)
SIGNAL				
0.0%	20.8	24.8	32.0	56.0
0.5%	30.4	36.0	48.8	76.0
1.0%	37.6	43.6	56.4	78.0
2.0%	48.0	54.0	66.0	88.4
QCD				
0.0%	7.2	7.6	8.0	12.8
0.5%	9.6	10.0	12.0	19.2
1.0%	12.0	12.8	14.8	24.4
2.0%	18.8	20.0	22.4	34.8

Table 4: *Total time necessary to process a given fraction of VH events of signal with $M_H = 120$ GeV/c^2 or of QCD background passing single tower trigger: single tower ≥ 10 GeV, as a function of the noise level.*

DOUBLE TOWER TRIGGER	t(85%) (μs)	t(90%) (μs)	t(95%) (μs)	t(99%) (μs)
SIGNAL				
0.0%	21.6	24.8	33.2	56.0
0.5%	31.6	36.4	49.6	76.0
1.0%	38.8	44.4	57.6	78.8
2.0%	49.6	55.2	66.8	89.6
QCD				
0.0%	7.6	8.0	9.6	14.4
0.5%	10.8	11.6	13.6	20.0
1.0%	14.8	16.0	18.8	33.2
2.0%	21.2	22.0	26.8	35.6

Table 5: *Total time necessary to process a given fraction of VH events of signal with $M_H = 120$ GeV/c^2 or of QCD background passing double tower trigger : 2 XFT tracks $p_T \geq 2$ GeV/c, and 2 central tower $E_{em} + E_{had} \geq 2$ GeV as a function of the noise level.*

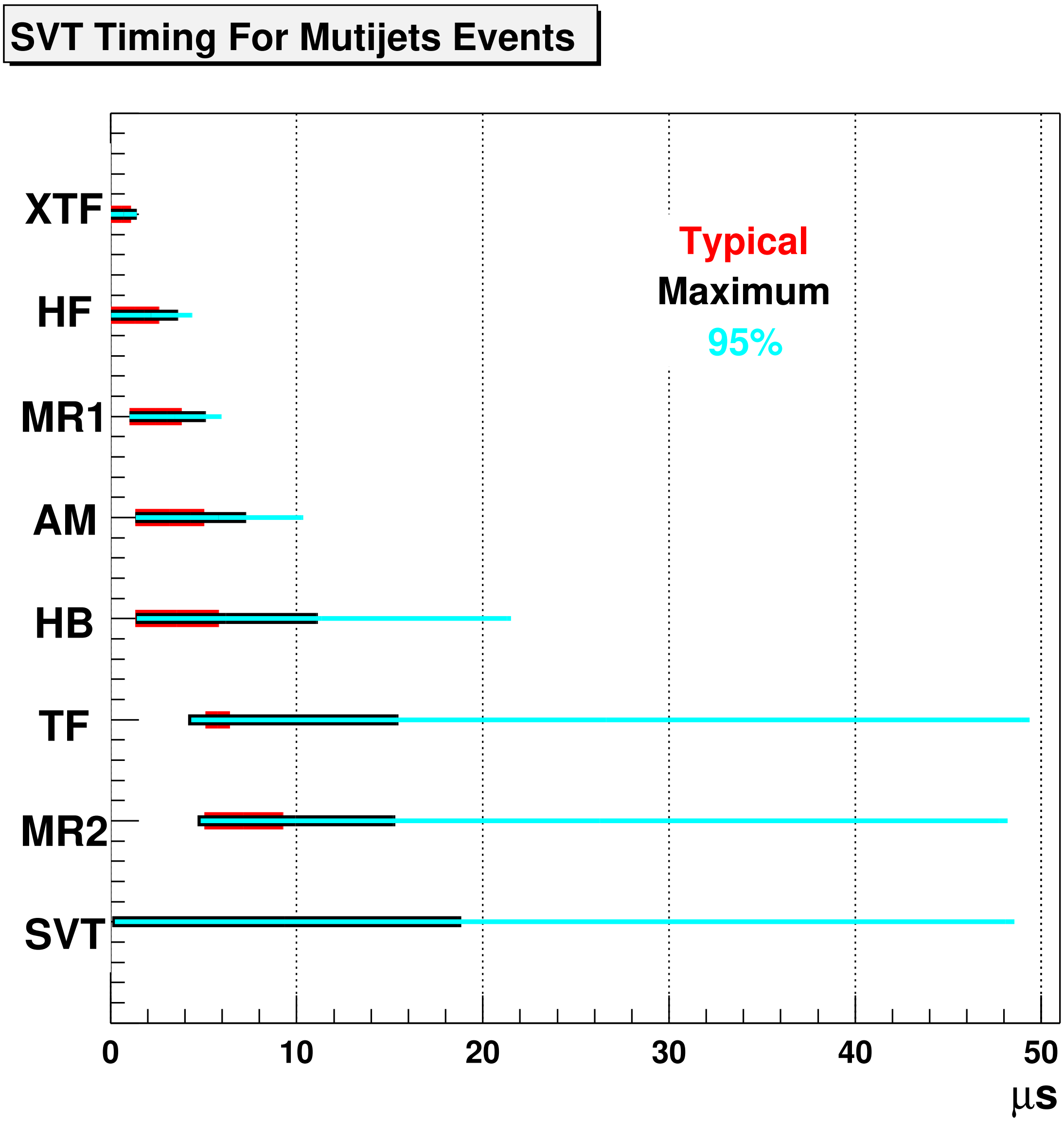

Figure 27: *This bar chart shows which SVT block is processing the data as a function of time from Level 1 accept. Each thick red bar has extrema at the average value of* t_1^{in} *and* t_2^{out} *(see text), while the blue bar extends to the minimum and maximum of those values among the 12 parallel streams. The thin magenta line extends to the point when events have a 95% chance of having been finished processing from each block. A 0.5% electronic noise and single tower trigger have been used.*

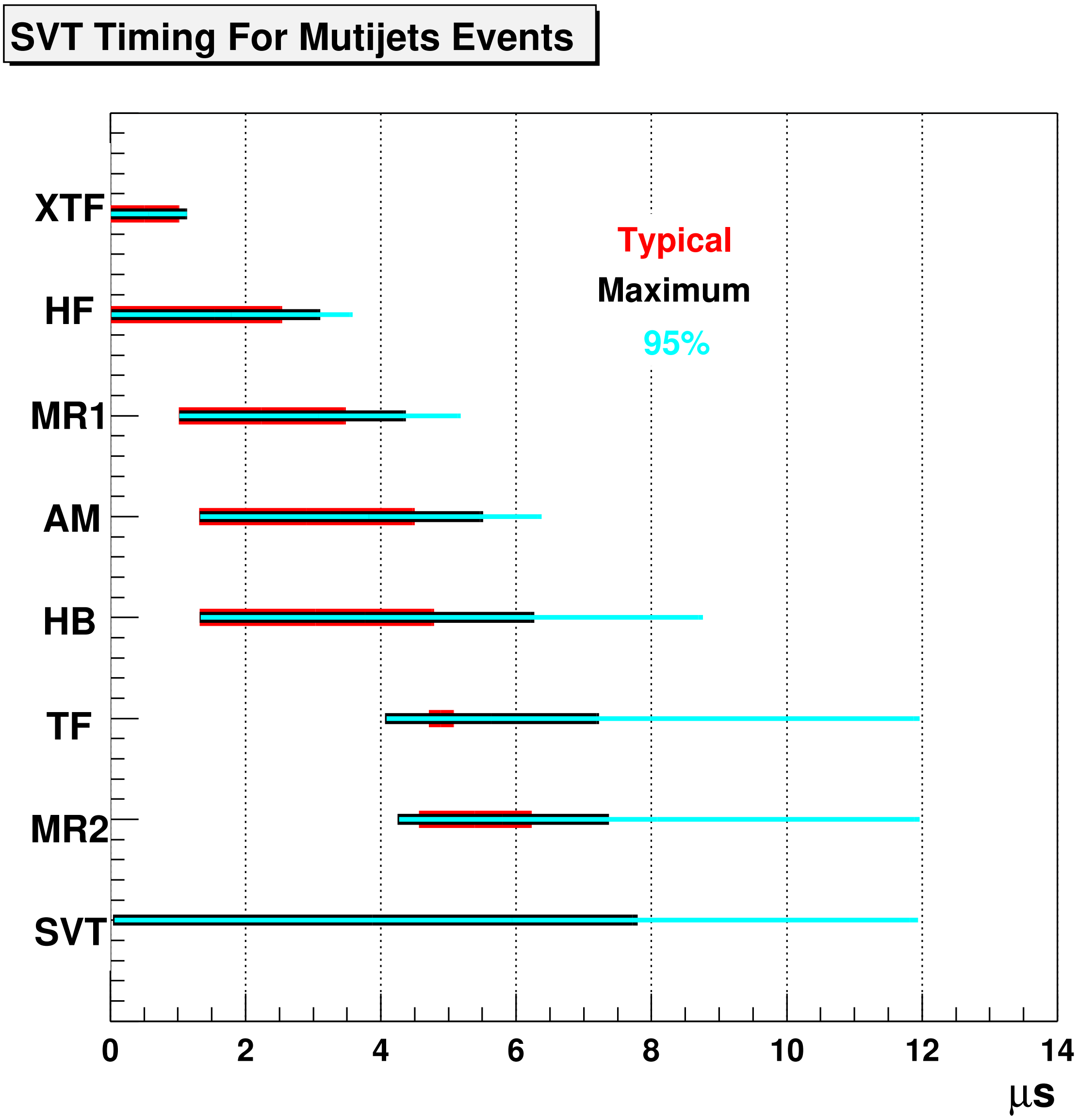

Figure 28: *This bar chart shows which SVT block is processing background events as a function of time from Level 1 accept. Each thick red bar has extrema at the average value of* t_1^{in} *and* t_2^{out} *(see text), while the blue bar extends to the minimum and maximum of those values among the 12 parallel streams. The thin magenta line extends to the point when events have a 95% chance of having been finished processing from each block. A 0.5% electronic noise and single tower trigger have been used.*

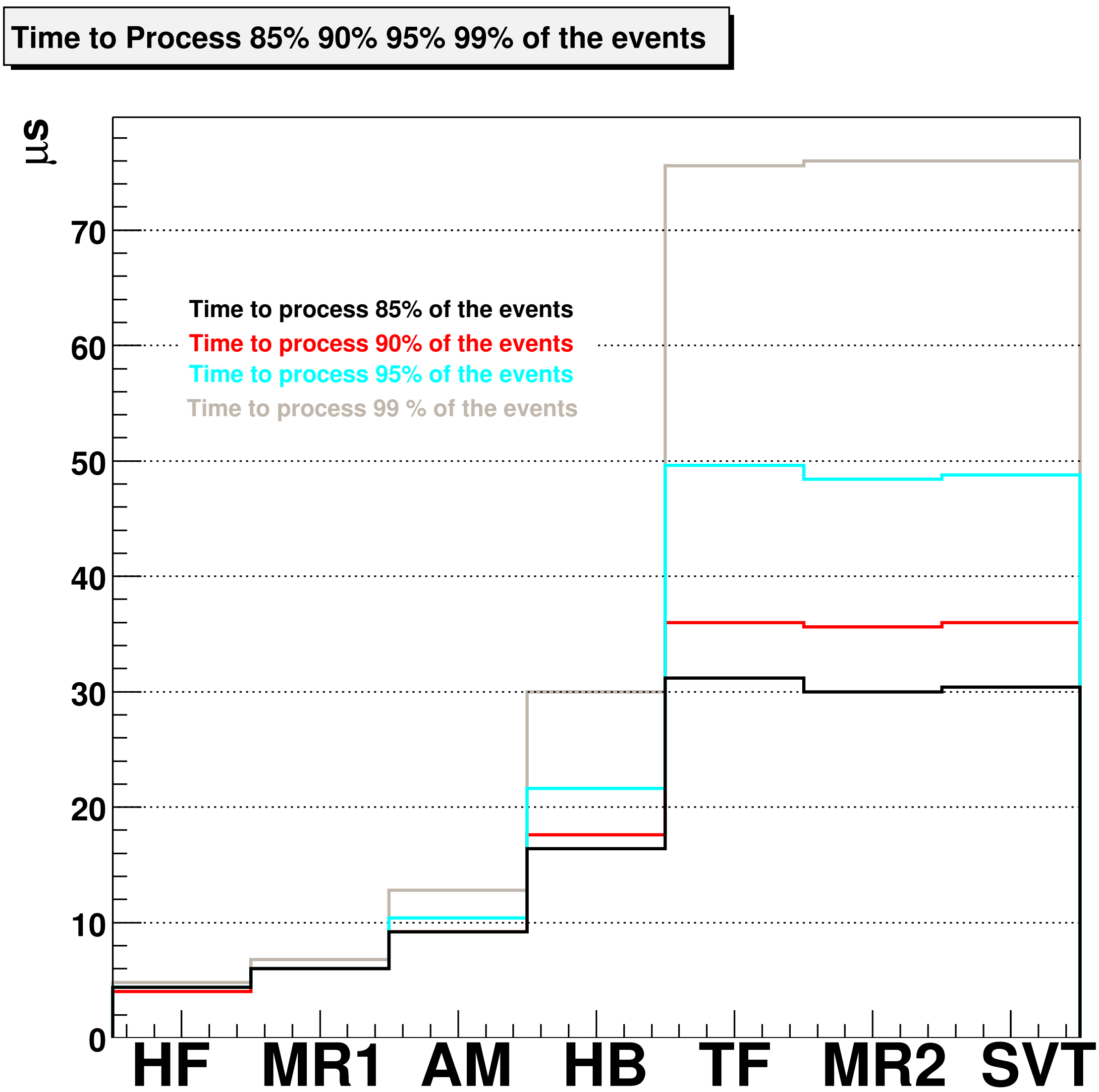

Figure 29: *Cumulative time necessary to process signal events through the various blocks of SVT a given fraction of the events. The default value of noise in the silicon strips and single tower trigger have been used.*

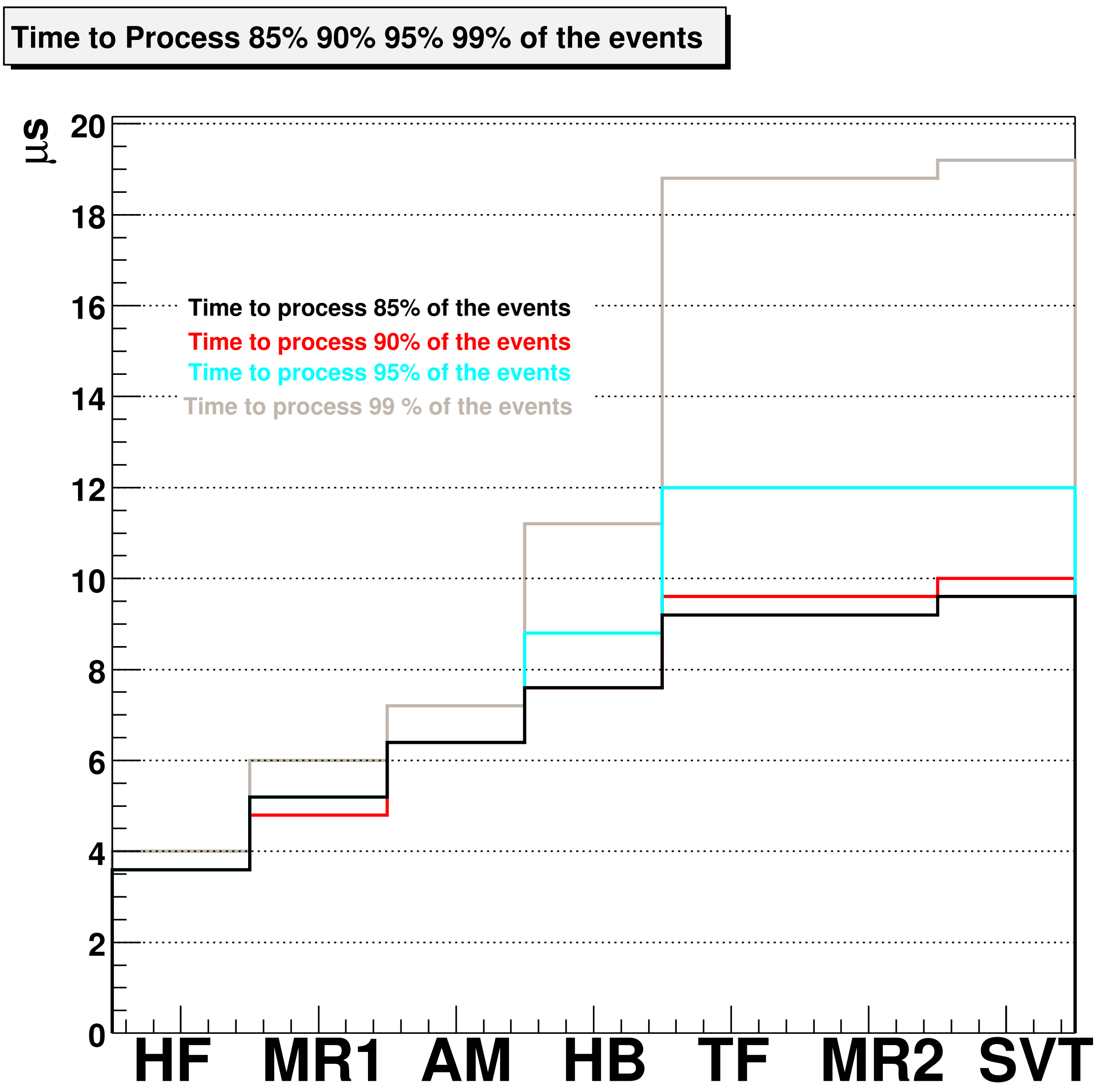

Figure 30: *Cumulative time necessary to process background events through the various blocks of SVT a given fraction of the events. The default value of noise in the silicon strips and the single tower trigger have been used.*

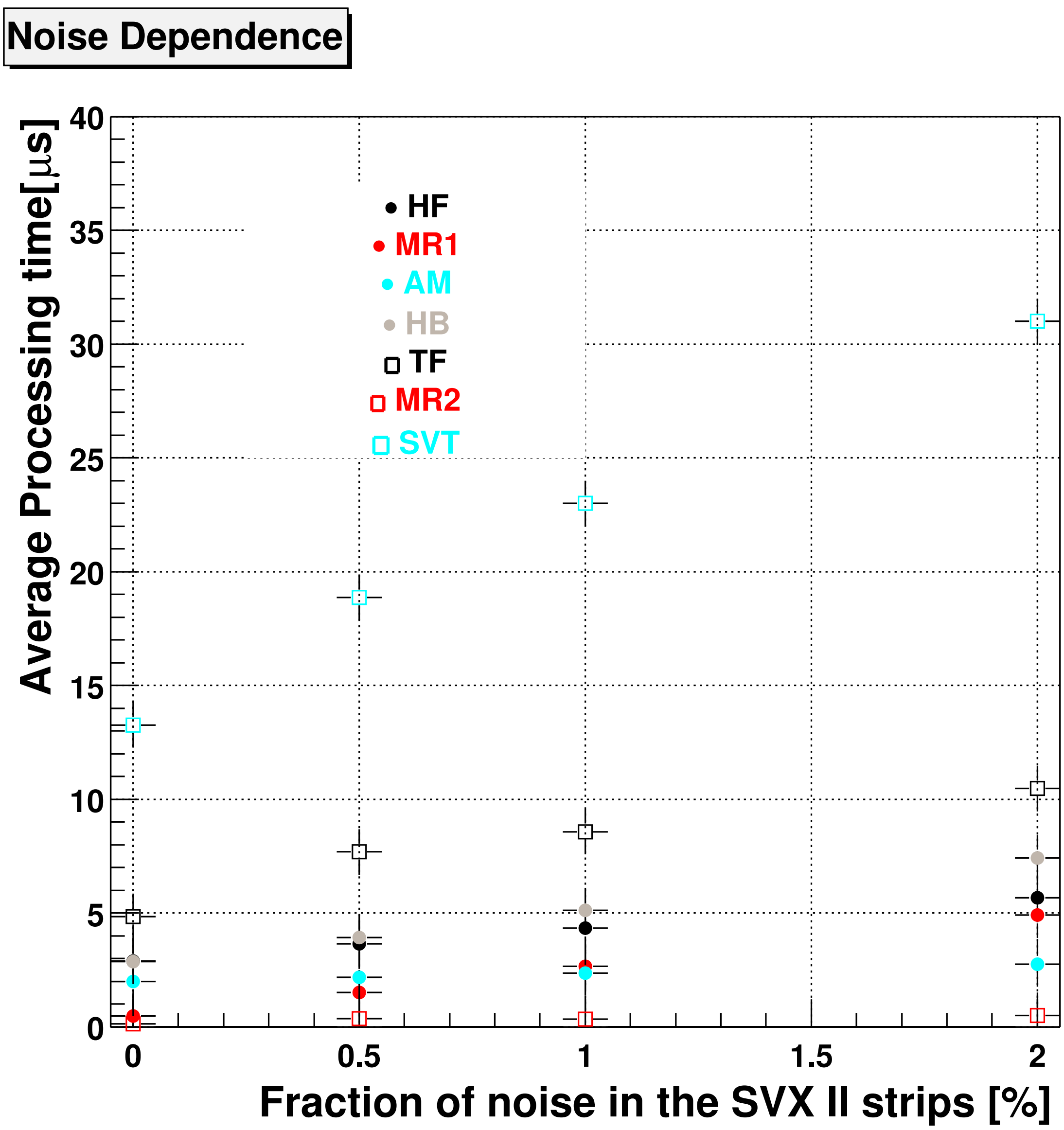

Figure 31: *Dependence of the average processing time of SVT on the amount of hits due to electronic noise in the silicon microstrips. Single Tower trigger has been used.*

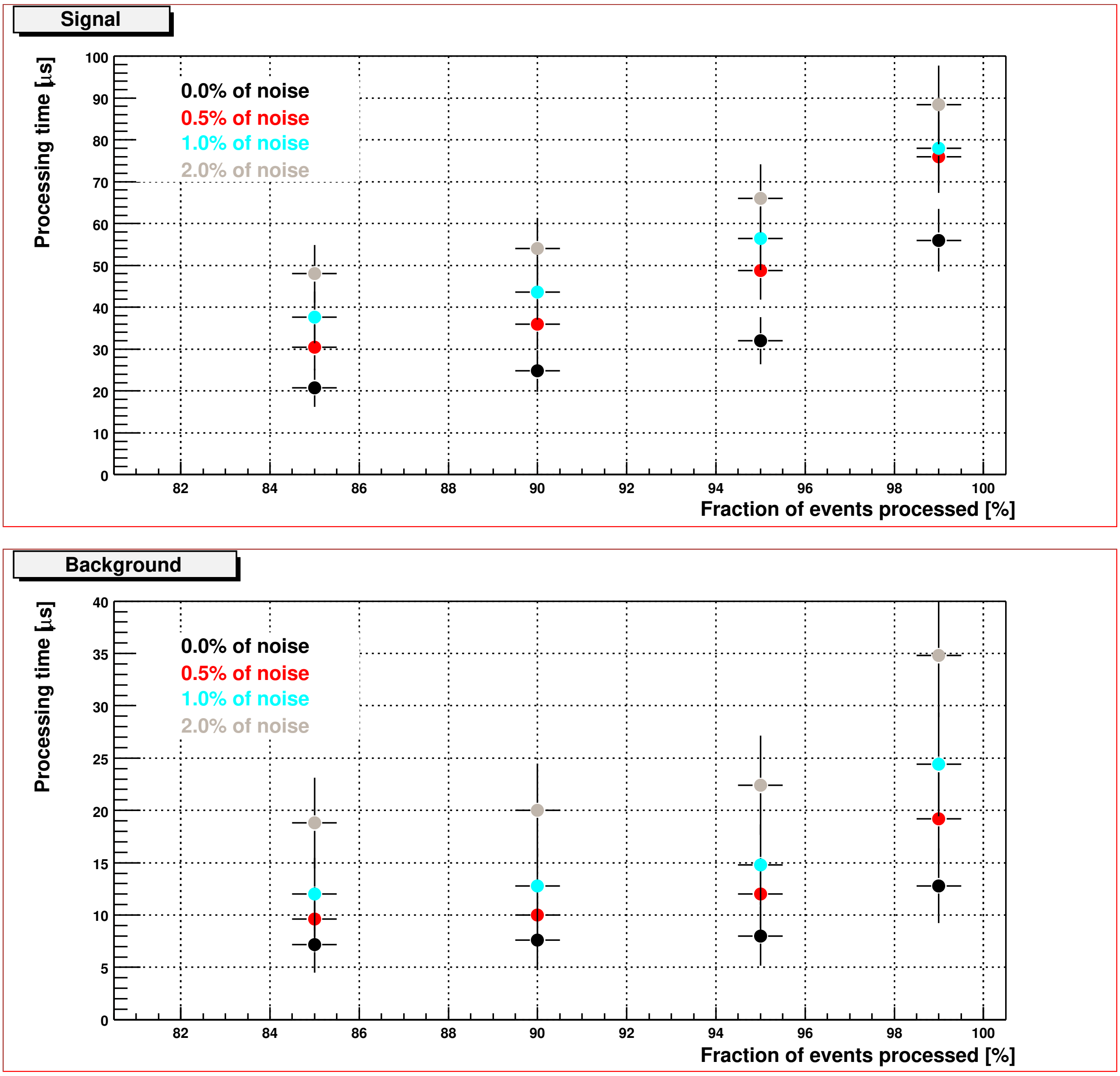

Figure 32: *These plots show the total time to process a given fraction of VH signal with $M_H = 120$ GeV/c^2 (on the top), and a given fraction of background events (on the bottom), as a function of the noise set on the silicon strips. Single Tower trigger has been used.*

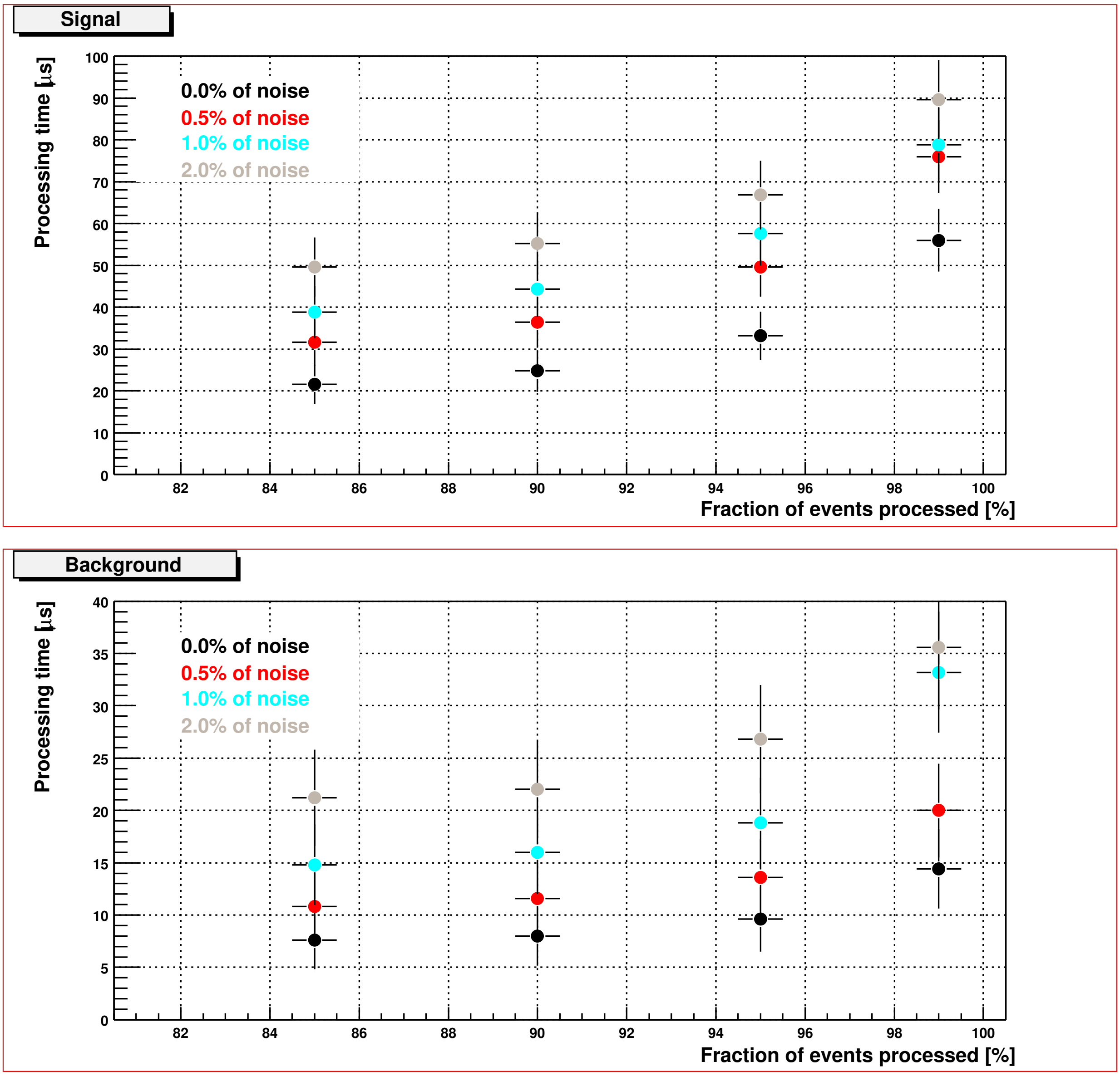

Figure 33: *These plots show the total time to process a given fraction of VH signal with $M_H = 120\ GeV/c^2$ (on the top), and a given fraction of background events (on the bottom), as a function of the noise set on the silicon strips. Double tower trigger has been used.*

5 Level 3

The guiding idea for the Level 3 selection consists of exploiting the better resolution achievable by a more sophisticated event reconstruction, which allows a more discriminant b-jet identification. This will be combined with more stringent calorimetric requirements.

5.1 Calorimetry

At Level 3, calorimetry requirements essentially are aimed at confirming the Level 2 requirements; this, in particular, means that events passing Level 3 should have at least 3 jets[14] with a minimum transverse energy of 10 GeV. Similarly, there will be a requirement on ΣE_T^{jet}, but the value of the cut should be decided only after the b tagging requirements in order to keep control of the rate.

5.2 b-jet identification

b-jet identification al Level 3 has not been studied in detail yet. Actually, the currently available tracking simulation does not allow very sophisticated studies so far. However, the low rate level we obtain at Level 2 will allow to apply very loose requirements (or just Level 2 confirmation) at Level 3. These requirements should be aimed at producing a high purity subsample of 4-jet data with SVT without tags, necessarily discarding the large dataset in output from Level 2.

Another possible approach has been studied in Ref. [5], where a soft lepton is required at Level 3, after the Level 2 calorimetric trigger. Such a strategy has been shown to allow the collection of 18% of signal events at a rate of about 1.43 Hz.

6 Summary

The possibility to contribute to a Higgs boson discovery in Run II with the 4-jet decay channel of associated VH production, and the usefulness of a multijet dataset in the search of several other supersymmetric signatures, are a strong encouragement toward trying to understand what is the best way to collect a multijet dataset enriched in heavy flavor decays, particularly given that the Run I multijet trigger yielded a very poor collection efficiency for all these processes[6].

In order to use the powerful SVT information at trigger Level 2, we need to ascertain that the impact parameter of charged tracks can be effectively measured in crowded, high-P_T 4-jet events, and that mismeasured tracks in QCD background events do not spoil its discriminating power. Furthermore, an optimized selection at Level 2 should be based on quantities insensitive to experimental conditions, such as noise level in the silicon strips. Finally, the processing time of these complicated events needs to be studied to ensure that the SVT output can be used by the Level 2 processors.

A selection requiring some calorimetric requirements and two SVT tracks with impact parameter larger than 100 μm appears a stable, conservative method to collect heavy flavor

[14]Jets are reconstructed with a cone $R = 0.4$

decays; events thus collected should have a very high probability of being tagged by an offline secondary vertex identification algorithm, while background is reduced at 1.5 Hz. A larger-than-estimated amount of noise in the silicon microstrips does not seem to have a large impact in the effectiveness of this selection criteria, although it does produce a non-negligible increase in background rates. In those conditions, if rates become an issue, a stricter cut on the fit χ^2 of SVT tracks (lowered from 12.6 to 10 or even 8) could be considered a valid choice.

It appears critical to perform a cleanup of the set of identified SVT tracks to reject multiplets of fakes extrapolating to the same XFT slice on COT superlayer 6. Given the availability of the information on the XFT seed of each found SVT track, we propose a very simple prescription for that task, which performs very well in our simulations; however, the possibility of implementing it needs verification. In the absence of such a cleanup, the effectiveness of impact-parameter-based selections on multijet events seems dubious.

Multijet events take on average 8 μs to be tracked by SVT; this number depends strongly on the noise level in the silicon. The distribution of processing time has long tails: these imply that a cutoff in the time available to SVT before a decision is taken by the Level 2 processors would have a dangerous impact on the efficiency on VH events, which take ~ 76 μs to be tracked at 99%.

An open question is whether a different set of SVX planes in input to SVT can improve the present picture. Also, the use of a different superstrip size on the fly, when analyzing events that fired a calorimetric Level 1 trigger, should be investigated.

7 Acknowledgements

Most of the present work is based on code written by G. Punzi (the SVT standalone simulation), P. Gatti (the dumpSVT module), and G. Chlachidze (the timing model). We are thankful for their help and for many useful discussions and clarifications.

References

[1] M. Carena, J. S. Conway, H. E. Haber, J. D. Hobbs *et al.*, (The Fermilab Higgs Working Group), *Report of the Higgs Working Group*, HEP-PH/0010338.

[2] S. Donati *et al.*, *Performance of SVT during the Commissioning Run*, CDF internal note 5511.

[3] S. Belforte *et al.*, *Silicon Vertex Tracker Technical Design Report*, CDF internal note 3108.

[4] A. Ribon *et al.*, *Charge Deposition Model in Silicon*, CDF internal note 5080.

[5] P. Azzi *et al.*, *A Run II Soft Lepton Tag-based Trigger for $H^0 + V$*, CDF internal note 5485.

[6] J. Troconiz, J. A. Valls, R. Vilar, *Update in the Search for a Neutral Heavy Scalar in the Multijet Data Sample*, CDF internal note 4129.

[7] M. Albrow *et al.* (The CDF Trigger and Datasets Working Group), *Run-II Trigger Table and Datasets Plan*, CDF internal note 4718.

[8] A. Clark and X. Wu, *High P_T b-jet Trigger for Runb II*, CDF internal note 4901.

[9] S. Belforte *et al.*, *Specification of the XTRP, SVT, and Level 2 Interfaces*, CDF internal note 4578.

[10] G. Busetto, D. Lucchesi, G. Punzi, *Performances Comparison of SVT in the Baseline Configuration and with Layer 00* , CDF internal note 5134.

[11] G. Chlachidze, V. Glagolev, G. Punzi, *Timing for the SVT Trigger*, CDF internal note 5021.